**Australia**

**Response surface methodology**

**Submitted by**: Aziz Alawad

0061022459

**Supervisor**: Belal Yousif

In fulfilment of the requirements of

**ENG-4111&4112** research project part 1&2

Towards the degree of

Bachelor of Mechanical Engineering (BENG)

# Abstract

There has been a great interest throughout the past years, in using the natural fibres to reinforcement the polymeric composites. A comprehensive study of the tribology science of the fibre composites is essential to ensure its capability to stand any given task. The main objective of the research is to obtain empirical equations for the temperature and friction of the studied Kenaf fibre. Minitab software was implemented in the research to conduct all the needed tests also to produce the figures.  The key findings of this research are that, the frictional behavior of composites has a high frictional coefficient at the begging of the tribology test because of the high shear force in the contact zone, friction coefficient and temperature increases when the applied load is increased, friction coefficient decreases with the increment of the rotating speed and the high influence of rotating speed on temperature so that temperature increases when rotating speed increases, in other words temperature will increase 5 $c^o$ for every 0.1 m/s increment in the rotating speed.

## Certification of Dissertation

I certify that the ideas, designs and experimental work, results, analyses and conclusions set out in this dissertation are entirely my own effort, except where otherwise indicated and acknowledged.

I further certify that the work is original and has not been previously submitted for assessment in any other course or institution, except where specifically stated.

Alawad, Aziz

0061022459

# Acknowledgement

I would like to thank my supervisor Dr Belal Yousif for his continues help and advices throughout my project. I'm practically grateful for my Mom and Dad for always being in my life. Advices giving by my sister Ghadah have been a great help throughout my studies in Australia and I wish to thank her for her never ending care and support. My special thanks are extended to my friend and niece Haya for her continues encouragement and support.

# TABLE OF CONTENTS

## CONTENTS

# LIST OF TABLES

# LIST OF FIGURES

# CHAPTER 1

# INTRODUCTION

## 1.1 Introduction

In many cases, the researchers wish to improve the performance or the result of an on-going system without stopping the system from working and just by changing the values of the parameters that control the output of the system. To do so, an exploration of the region where these parameters are varied is needed. This includes two steps, first is to examine some of the points in the region and to achieve the results. Secondly, is to make an estimation of the results that would be found in rest of the points by relying on the reliability of this estimation. Now, the researchers should know whether the system's result can be improved or not. Furthermore, the researchers will be able to know to what level the system can be improved and the exact parameters that should be used to make this improvement, (Ortiz et al., 2009).

The response surface methodology (RSM) can be defined as a collection of statistical and mathematical techniques that is used in the aim of developing an adequate functional relationship between a number of inputs (variables $x_1$, $x_2$, $x_3$, $x_n$)

and an output (response *y*). Generally, the relationship between the response and the variables is unknown however; it can be approximated using a low degree polynomial, (Khuri and Mukhopadhyay, 2010). For instance, the growth of a plant is relying on the amount of water the plant receives ($x_1$) and the amount of sunshine the plant exposes ($x_2$). Under any combination of $x_1$ and $x_2$ the plant will grow.

If there is a continuous range of values for the variables as well as for the response, respond surface methodology is very useful for optimizing the response value. In this example, the independent variables are $x_1$ and $x_2$ and the response (y) is the plant growth and the function is expressed as:

$$y = f(x_1, x2) + \varepsilon$$

Where; y is the response variable which depends on $x_1$ and $x_2$ which are the independent variables. The term $\varepsilon$ represents any other source of variability not included in the function $f$. Thus $\varepsilon$ includes the response measurement error, vibration and the error in the independent variables. So, in the above equation $\varepsilon$ is treated as a statistical error with zero mean,(Myers and Anderson-Cook, 2009). Generally, the response function ($f$) for the majority of RSM problems is unknown. To come up with good approximation, the researchers often start with a low-order polynomial under (Rabinowicz, 1965)a small region. The approximated function is said to be a first-order polynomial if the response (y) can be defined by a linear function in term of its independent variables ($x_1$ and $x_2$). The following expression shows a first order-polynomial with three independent variables (a, b, c);

$$y = \beta_0 + \beta_1 a + \beta_2 b + \beta_3 c + \varepsilon$$

A second-degree polynomial is appropriate to be used for the approximation, if there is a curvature in the response. A second-degree polynomial with three independent variables (a, b, c) can be expressed as follows;

$$y = \beta_0 + \beta_1 a + \beta_2 b + \beta_3 c + \beta_4 ab + \beta_5 ac + \beta_6 bc + \beta_7 a^2 + \beta_8 b^2 + \beta_9 c^2 + \varepsilon$$

All RSM problems generally use either the first degree polynomial or the second degree polynomial or a combination of them both to establish a relationship between the response (y) and regressions ($x_1$, $x_2$, $x_3$….$x_n$). An appropriate experimental design must be used to collect data to get an efficient approximation of the polynomial. There are three basic methods for collecting data which are ,(Myers and Anderson-Cook, 2009)

- A retrospective study based on historical data.

- An observational study.

- A designed experiment.

Good data collection will help in simplifying the analysis and presents more applicable models. On the other hand, bad data collection can cause problems in the analysis and its interpretation. After collecting the data the method of least square is to be used to estimate the polynomial's parameters. The Method of Least Squares is a technique applied in the determination of the best line that fits to data, where its theory of proof applies simple linear algebra and calculus concepts, (Larson and

Farber, 2006). However, the primary challenge is when finding the best fit straight line.

In the current research, a literature review is conducted with a primary objective of learning about three basic concepts of design optimization in the moving parts of machinery with respect to their relation to response surface methodology; First, Tribology Science conception is reviewed and its basic relation to the topic is discussed. Second, the paper reviews about Friction in general and its relation to the topic, and lastly, the science of Adhesion Wear in polynomials and design experiments in machinery is also discussed. The purpose of the review on the above areas will create more information about the approaches to minimization and elimination of losses that result from friction and wearing of machinery or moving parts at all levels of technology where surface interaction and rubbing are often elaborate. The current research is aimed at leading to better performance, increased systems efficiency, significant savings, and fewer breakdowns.

## 1.2 OBJECTIVES

The aims of the project are:

1. Search and learn about the background and applications of the response surface methodology (RMS) ans how to apply it on the experimental data.

2. Analyse the experimental data using the (RSM) to develop a relationship (equation) between the response and the independent variables.

3. Form this research an empirical equation will be developed and used as a base for the researchers.

## 1.3 CONTRIBUTIONS AND SIGNIFICANCES

The findings of the current study will contribute to:

- The outcome of this research will contribute to the knowledge of tribology since, there is lack of work in the responds surface area .

- The outcome of the work will be published in an international journal related to the area of study.

- Using Minitab Software in this research will help the researchers in saving time and money doing such a study.

## 1.4 THESIS LAYOUT

The figure 1 below shows the layout of the thesis. The thesis consists of 5 chapters; introduction, background knowledge and literature review, methodology, results and discussion and conclusion and recommendations.

**LAYOUT OF THE THESIS**

| | |
|---|---|
| CHAPTER 1 | Introduction |
| CHAPTER 2 | Literature review |
| CHAPTER 3 | Methodology |
| | Collecting the exp. Data |
| | Analysing the data using Minitab |
| | Extract the main findings of the simulation |
| CHAPTER 4 | Results and discussions |
| CHAPTER 5 | Conclusion |
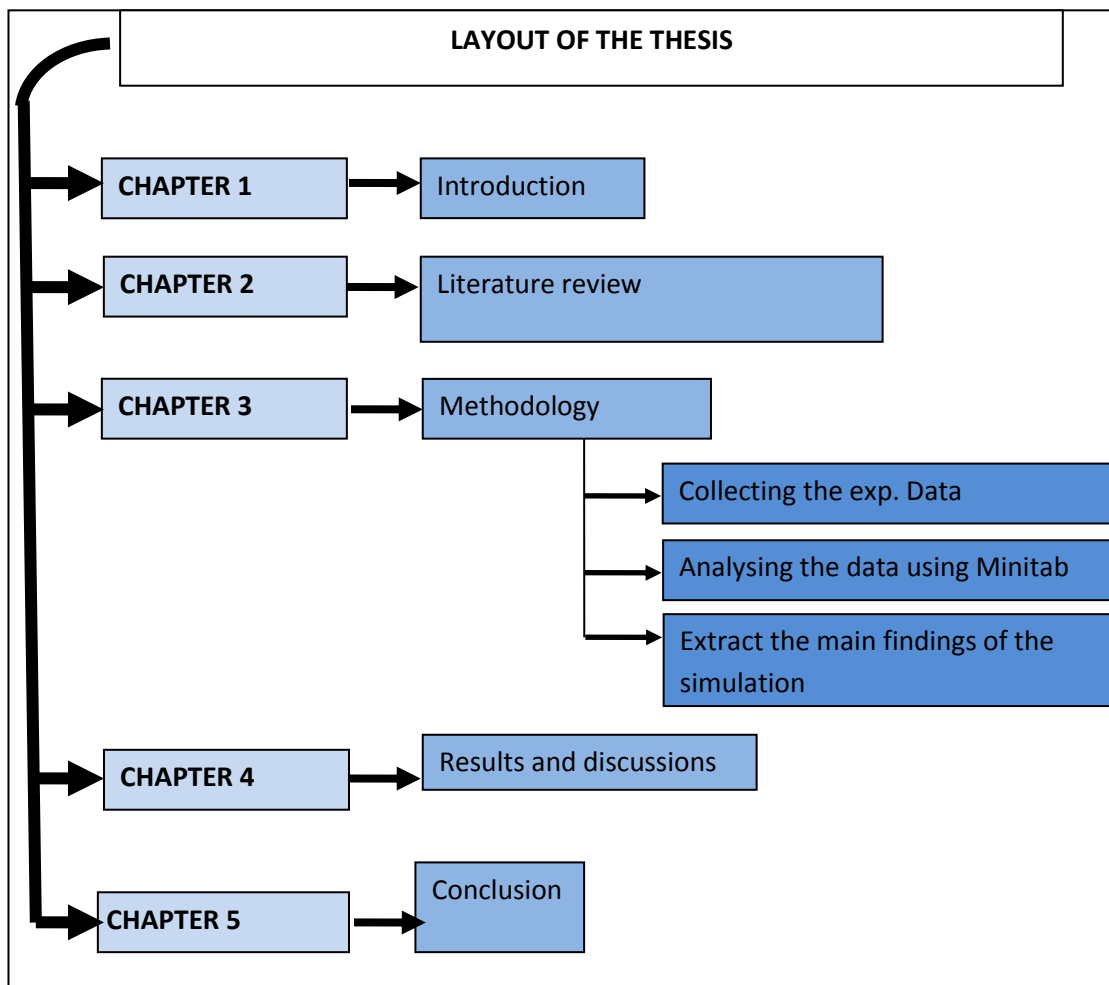
Fig.1. 1 The layout of thesis

# CHAPTER 2

# LITERATURE REVIEW

## 2.1 Applications of RSM

In statistics RSM is widely applied in defining a mathematical relationship between one or more variables and a response or multiple responses. In today's industrial world RSM is used in many applications due to its cost effectiveness and time effectiveness in analysing the scientific studies as it offers reduce in cost and time in comparison with the other scientific analysis methods such as lab experiments. RSM is used in many different scientific fields such as chemistry science, social science, engineering science and formal science. The method of RSM was first introduced in 1951 by G.E.P. Box and K. B. Wilson. The idea is to make estimation for the response using a low degree polynomial either first degree polynomial if there is a linear relationship or second degree polynomial if the relationship is curvature. Although the first estimation would not be accurate, however it will give an overview of the relationship between the response and the variables and how the response would vary or behave with the variables.

In statistics, there is an important aspect of RSM where it is used as a statistical technique and as a mathematical approach to empirical model building, (Box and Draper, 2007). Through the application of careful design models, it is possible to

obtain efficient machinery parts where the primary aim is to boost a given response (output variable) for example increasing machinery efficiency and reduction in drag force of friction, (Larson and Farber, 2006). Output variables are often affected by a number of independent variables which are often adjusted through a series of experimental data and the input variables subsequently regulated to identify how they affect the output response, (Cornell, 2011).

## 2.2 Formulation models

Initially, the development of RSM was initiated with an aim of developing empirical responses before being adopted later in numerical experiments to formulate models. The variance is in the type of error produced by the anticipated response. For instance, in designing physical experimentations, measurement errors may be the cause of inaccuracy, while in computer trials incomplete convergence of discrete representation, round-off-errors, or iterative processes, usually results in numerical noises in a continuous physical activity, (Roux et al., 1999). In response surface methodology, the assumption taken is that, all errors to be random. In this review, the application of RSM to machinery design optimization is focused at decreasing the costly analysis techniques, such as CFD analysis and finite element method, and their concomitant numerical noise ,(Bigoni, 2012). The problems can be estimated as described in the review with polynomial functions that can increase the convergence of the optimization procedure because they decrease the outcome of noise and they permit the application of derivative-based procedures. There are many benefits associated with using response surface method for design optimization applications.

For instance, when optimizing machinery in order to reduce friction and adhesion between the interacting surfaces that are in relative motion, an engineer may be compelled to search for the relationship between parameters that control the output of the system such as the applied force (x1) and the sliding velocity (x2) that usually accelerate the wearing rate (y=response outcome) of machine parts. The wearing of machines (response) as a function of the amount of applied force and sliding velocity (variables) can be represented as follows:

$$y = f(x1, x2) + \varepsilon$$

Where $\varepsilon$ represent the error or noise that is detected in response y. Therefore, the interacting machinery planes where the wearing phenomenon is detected can be represented by the function $f$(x1, x2) which is its proportional or direct response surface, (Wu and Hamada, 2000).

The above response can be symbolized graphically, either in a contour plot version or in a three dimensional space. This approach helps in visualizing and easing the perception on the shape of the achieved response surface. In most instances, contours are curves that indicate a constant response that is drawn from x1, x2 planes while holding other variables at constant, (Oehlert, 2000a). Moreover, each contour is designed to correspond to a specific height of the response surface, as shown in Figure 2.1.
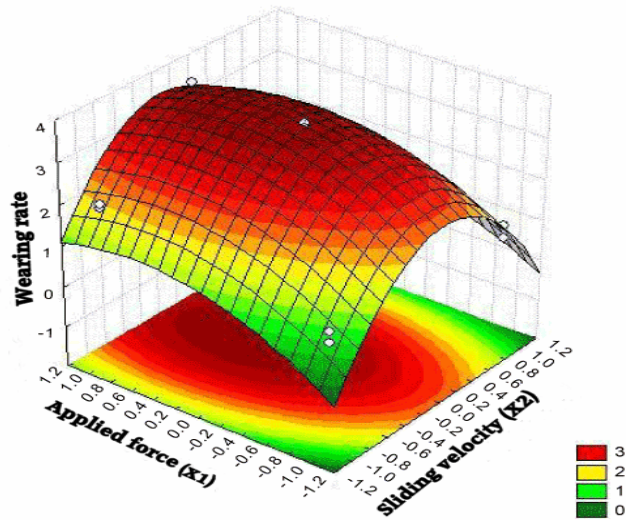
Figure 2. 1 Three-dimensional response surface and the corresponding contour

(Poggie et al., 1994).

The figure is plot for the interacting machine surfaces; where x1 is the applied force (N) and x2 is the sliding velocity (m/s) with respect to how they contribute to wearing rate of machine.

Given the above elaborations, it is clear that RSM can be used in design analysis making this review important in relation to machinery designs focused at reducing friction and increasing efficiency. Therefore, it will be important to gain a background understanding and what previous scholars have discussed concerning the topic as discussed in the subsequent sections below.

## 2.3 Tribology science

Tribology is a discipline and technology of friction, material wearing, and surface lubrication of interacting surfaces in a relative motion, (Majumdar and Bhushan, 1990). Besides, tribology looks into aspects related to adhesion, mechanical properties, and coating of engineered planes. This scope includes modelling of statistic (adhesion and indentation), experimental investigation dynamic contacts (rolling, scratching, oscillating, and sliding), and fracture or contact mechanics throughout several length scales ranging from macroscopic to atomistic scopes, (Ruan and Bhushan, 1994).

## 2.3.1 Importance of Tribology

Current contributions to advance mechanic and scientific comprehension of mechanical response and tribology performance of engineered coatings and surface have been reported to have a significant contribution in coating design and establishment of precise applications with increased efficiency,(Stachowiak and Batchelor, 2011) .Special attention has also been placed on characterization of mechanical properties and tribology of structure versus property process and how they relate to engineered surfaces and their coatings. All materials have also been a centre of interest but more focus is based on multifunction materials (in terms of their lubricious and hardness) and Nano composite features for extreme environments, (DeGarmo et al., 2003).

Approaches noted above indicate that tribology has become a vital modern technology as far as machinery design of rolling and sliding surfaces are concerned. In tribology, some of the examples of productive wear include polishing, machining and writing with a pencil. (Jin et al., 1997) On the other hand instances of productive friction include application of driving wheels, nuts, bolts, clutches, and brakes. However, unproductive wear that remain the centre of concern is mostly attributed to cases such as seals, ball bearings cams, gears, and internal combustion. Estimates that result from unawareness about tribology sum up to 6% or $200 billion in losses per year,(Bhushan, 2001) .In addition, the world estimation in losses is about 1/3 in energy resources that is lost to friction in various forms. Therefore, understanding tribology subject is important in ensuring effective wear control and friction reduction while at the same time prolonging the reliability of engineered designs. (Kuhn et al., 2003) had argue that approximately 200 billion dollars can be saved across the world per year if industries adopt appropriate tribology practices .With this remark,(Jin et al., 1997) had earlier pointed out that better tribology designs will contribute to enormous savings, and that this can be achieved without deploying huge capital investments.

In engineered designs, three primary areas of importance of tribology focus are attributed to adhesion, lubrication, and wear which are often documented with reference to atomic focus on the moving sections. Adhesive concept, as later discussed, is important in the success in various applications but currently there is no systematic model present in predicting adhesion between various material elements,

(Box and Draper, 2007). Alternatively, engineers have found it appropriate to employ electronic structure approach in examining adhesion between material elements of curiosity, for instance, application of ceramic in determining factors that catalyze friction between two moving surfaces or how adhesion is controlled, (Cornell, 2011).

In addition, the used lubricants in friction control should comprise boundary additives to join the surface and the lubricant more strongly in such a way that at when higher pressure or stress is applied, the rate of wear between two opposite surfaces is reduced, (Cornell, 2011). To date, little has been documented with regard to how boundary additives adhere to surfaces of metals and how electronic models are used to investigate this phenomenon in polynomial relations. Regarding surface wearing, engineers mainly focus on the tribology of molecular dynamic simulation in relation to indentation and erosion with regard to loading rate, temperature and interaction effect, (Kuhn et al., 2003). In polynomial relations, tribology becomes critical in developing engineering equations, methods and formulae in general application of engineering design, (Bhushan and Gupta, 1991). Even so, a number of useful equations and methods exist and mostly in contact stress calculations and in fluid lubrication estimations.

## 2.3.2 Modelling of Tribological Behaviour of materials

Given that friction and temperature play an important role in defining and shaping of models, various variables may be required in estimating the rise in temperature on sliding surfaces. On the contrary, a greater number of variables are often needed in designing of appropriate wear and friction properties of sliding surfaces,(Holmberg et al., 1998). Shortage of appropriate design approaches for realizing anticipated product quality and friction life practically always results in delaying these contemplations in merchandise development until meagre days remain before manufacture deadline ,(Jones and Scott, 1983).

At this point, tribology equations are formulated to ensure that first selections are completed in terms of designing shapes, processes and materials. Therefore, the early challenges are solved first including cost, method of production, features related to vibration, strength and product weight. This approach becomes problematic because the engineers rely on knowledge based on wearing and friction of the material prompting designers to result in guesswork and subjective information from the dealers of various products including materials and lubricants. Such randomly adopted frameworks and accelerated trials are inappropriate benchmarks towards realizing engineering design goals,(Roylance, 2003). Moreover, this approach has profound effects on the warranty costs of friction problems and the anticipated life of a design resulting in product failure in a number of mechanical, automobile, and other related industries,(Bhushan).

Ultimately, it is clear that tribology is a fundamental subject that requires a wide allied background of various subjects. In academic relations and engineering of product designs, primary engineering fields major on fluid mechanics elastics, material science, dynamic designs, and heat transfer in mechanical models,(Wu and Hamada, 2000).On the other hand, material engineering students tend to gravitate towards this tribology challenge by studying viscosity of plastics in relation to oxidation, adsorption, adhesion, surface chemistry, fracture strength, creep, lubricant chemistry and layer coating. The approach indicates the diversity of tribology science and technology in relation to engineered designs, (Diniz and Martin, 1996).

RSM is introduced in tribology to eliminate one factor after another deficit in demonstrating tribology characteristics between variables and response. This implies that by means of composite design model, there are few operating conditions required to institute the polynomial functions of applied load and sliding speed. A second degree polynomial can be applied to indicate how curved surfaces can fit in the empirical data. In addition to the findings related to operating conditions, the rate of wearing parameters and interaction temperatures gained from the polynomials are associated with the practical results. Tribology in the activation energy in the rate of wear is derived from a function of the applied load, sliding speed, and contact temperature in line with the model assumed by (Lin and Chou, 2002). Lastly, the data for the wearing rate constraint can be defined by smooth curves, in place of two different straight lines in binary temperature partitions—discussed later under adhesive wear in polynomials.

**2.4 Friction**

There are two primary types of friction forces; fluid friction and dry friction also called the coulomb friction. In fluid friction, the wearing force develops as a result of two layers that are moving at different velocities,(Hoyt, 1972). In contrast, dry friction occur as a result of rigid bodies that keep rotating on the surface of each other along a non-lubricated surface for instance in case of belt friction, journal bearing, thrust bearing, and squire-thread screws,(Goyal et al., 1991). In addition, the other forms of friction include lubricated friction where a fluid segregates two sliding surfaces, (Shaughnessy et al., 2005) another type is skin friction that takes place as a component of drag force that resists the movement of a body through fluid. Lastly, internal friction is a force that resists movement between the elements that make up the solid material as it undergoes deformation, (Batist, 1972).

In all industries, friction is attributed to causing wear and excess energy consumption. Globally, there is an estimated energy loss to friction thought to be around 30% to 50% in energy inputs facilitated at replacing worn out components and production costs. In RSM, formulas can be designed to improve structures designs with a primary focus of reducing friction wear and optimizing material output in system operations. Mechanical sliders, ball bearings, and corroding particles all enforce potentially detrimental circumstances upon the surface of its adjacent body on which it spins or rolls, whether the magnitude of events is microscopic or macroscopic. These effects include heating, strains, and modification

of chemical reactivity, each of which can act distinctly, however, each can also alter the rate of adjustment of other factors during a continued contact between two surfaces. The notion behind these observations argues that in the engineering appliances, there are no interacting surfaces that are perfectly frictionless. Rather, when two surfaces interact there is always a tangential force that will always develop in one respect to change any type of friction force: fluid friction of dry friction,(Oehlert, 2000b). The basic kinetic properties of sliding surfaces were discovered between the 15th and the 18th century and they were summarized into three practical laws, (Daniel et al., 1994).

- First is the Amonton's 1st law which states that friction force is directly related to the load applied.
- Amonton's 2nd law states that "the force of friction is independent of the apparent area of contact.
- The third law is Coulomb's Law of friction that states "Kinetic friction is independent of the sliding velocity.

**2.4.1 Dry Friction**

In dry friction, the force between to surfaces in contact is restricted from lateral motion with each other. In other words, the opposing surfaces are in static friction in relation to kinetic friction (also called dynamic or sliding friction) and the non-moving surfaces that revolves on the two surfaces, (Cook et al., 2010). The Coulomb

17

friction is suitable in calculating the dry friction force and it is governed by the equation below:

$$F_{\mathrm{f}} \leq \mu F_{\mathrm{n}}$$

Where: $F_{\mathrm{f,}}$ is the amount of exerted friction force by each opposite surfaces on each other. In other words, it presents a directionally opposite force parallel to the net force applied on the surface.

$\mu$: represents the friction coefficient, which is also the empirical characteristic of the materials in contact.

$F_{\mathrm{n}}$: represents the normal force that is exerted by the opposite surfaces on each other as a result of the normal or perpendicular force to the surface. Therefore, the Coulomb fraction which is $F_{\mathrm{f}}$ can take any value starting from zero up to the maximum possible value of $\mu F_{\mathrm{n}}$. Moreover, the direction of friction force against the opposite surface is parallel to the friction that any contrasting surface would experience, (Bigoni, 2012).

Dry friction defines the reaction between two solid surfaces in interaction with each other either in motion (kinetic friction) or when they are not (static friction) fig 2.2.
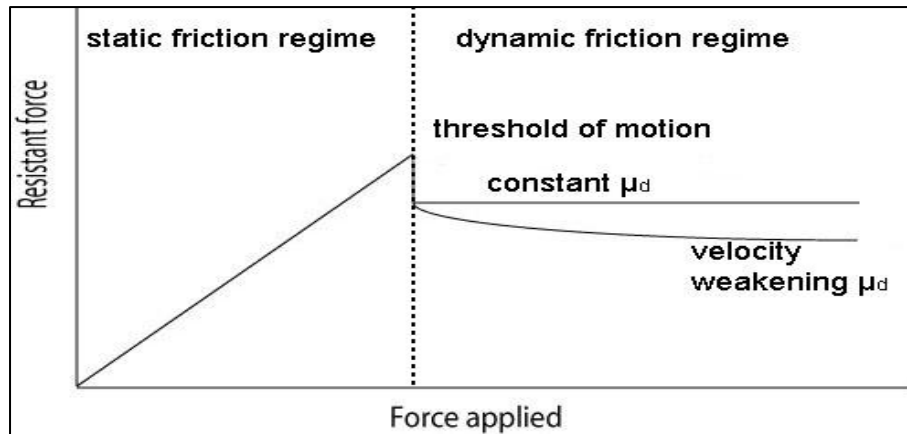
Figure 2. 2 Dry friction diagram in various states (Olsson et al., 1998)

Static and kinetic force and proportional to normal force between the interacting bodies and friction will work against the moving object. In fig 1, when an object is pushed it resists motion until the kinetic force is higher than that of friction force. When the force of friction is increased the body starts to move as friction force becomes kinetic friction and can either be constant with any velocity or can vary with velocity.

In static events, the dry force of friction is related to the force that must be applied in order to prevent the motion of two sliding surfaces; that it stabilizes the net power tending to cause such motion. Rather than giving an estimate of the definite frictional force, the Coulomb calculation offers a threshold assessment for this force, above which sliding movement would begin. This maximum pressure is acknowledged as traction force, (Simo and Laursen, 1992). The rubbing phenomenon can be explained by the Stribeck diagram (fig.2.3) in illustrating what occurs in lubricated

interactions. Friction coefficient linearly ascends for high values of η V/W because of the fluid lubrication; that is, it is related to viscous dragging within the oil film. As the viscosity and load increases, the η V/W factor falls. This makes the fluid to be thinner as the friction coefficient declines, up to a lowest value.
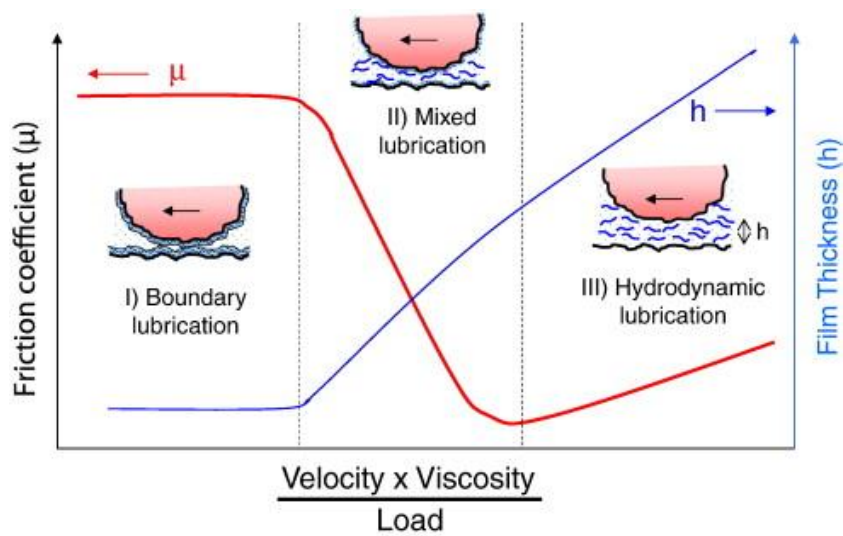


Figure 2. 3 Representation of schematic stribeck diagram: n-oil viscosity, V-sliding viscosity, W- normal load (Coles et al., 2010) .

Friction force is always applied in the direction that opposes motion (in the case of kinetic friction) while potential motion (in case of static friction) is applied to restrict motion between two surfaces. For instance, a curling rock that is sliding along the ice surface will experience a slow kinetic force that tends to drag the rock from motion. Another illustration is the potential motion in the driving wheel that accelerate the

car encounters a friction force that projects forwards, failure to which the wheels are most likely to spin while the rubber would slide backward in the opposite direction along the road surface. As such, the wheels do not oppose the direction of the vehicle in motion but they oppose the potential direction of sliding surfaces between the road and the tire (De Saxcé and Feng, 1998).

In summation, it can be pointed out that the force of friction acts in a course parallel to the contact area, while at the same time opposing the movement or the tendency of an opposite object to travel. The force friction is determined by two things:

- The normal force (Rn)
- The form of the surfaces involved ($\mu$), therefore,

  $F_{riction} = \mu \cdot Rn$

When the external force (F) is applied to propel a body initially the body fails to move, in these regard frictional force (f) drags the external force and resists it in the opposite direction and  that is because the frictional force is equal to applied force or F-f=0 . Therefore, the body continues to stay at rest and the force of friction is called static friction (fig.2.4).
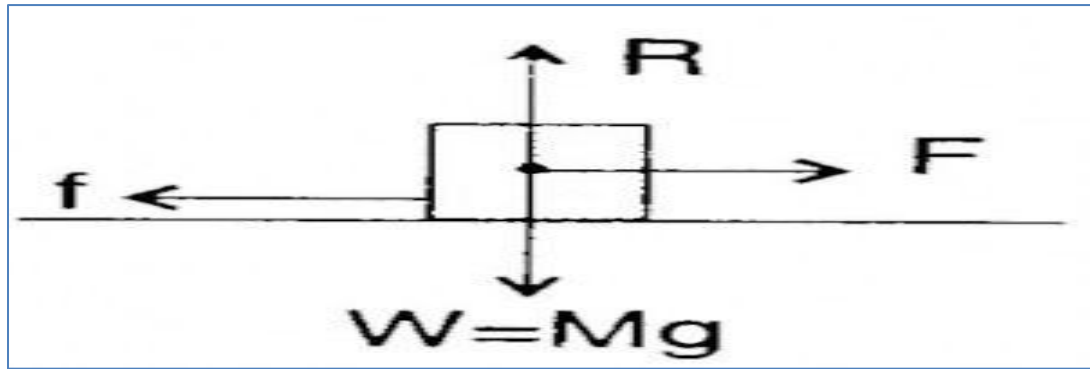
Figure 2. 4 Statistic friction(Poudel, 2013).

On the other hand, when external force (F) in increased further, the object draws close to the verge of motion, because the friction force is at maximum and this is called limiting friction with the equation: $f_s = \mu_s M g$

Where $\mu_s$ is denoted as the coefficient of static friction.

When the external force is applied beyond the limiting friction the body will start to move and the force limiting or opposing this motion is called sliding or kinetic friction. Kinetic friction is usually less than limiting friction.

**2.5 Adhesion wear of polynomial**

Clumps, aggregates or any group of atoms are mainly attracted to each other by various forces such as adhesion and cohesion. Atomic bonding is largely a result of

electron structure. The bonding between different materials is facilitated by adhesive forces. Where, the ultimate work of adhesion forces can be defined as the energy required for reversible separation or interaction between one interfaces with another surface, overlooking deformation. Though these dissipative processes command that the force required in an authentic cleavage experimentation continuously will be superior compared to the ideal force of adhesion (as a result of plastic distortion), the greater the force of adhesion, the more the required work that must be done to overcome the interface, (Lucas, 1994).

The adhesive force can be defined in terms of either the interfacial energies and the surface (relative to the particular bulk materials) or the dissimilarity in total force available between the interface and its isolated slabs. In engineering preparation, portions gliding against each other are frequently different. For instance, steel sliding on brass, without the presence of adsorbed layers, at times it may be speculated that the bonding system may result from ionic bonding, covalent, van der Waals forces or metallic bonds, (Watts, 1995). Adhesive wear results from breakdown of micro-junctions between opposing asperities on the rubbing surface of the interacting surfaces. The force of interaction applied becomes high and deforms the atomic interactions between the joints resulting to rupture and dissociation.
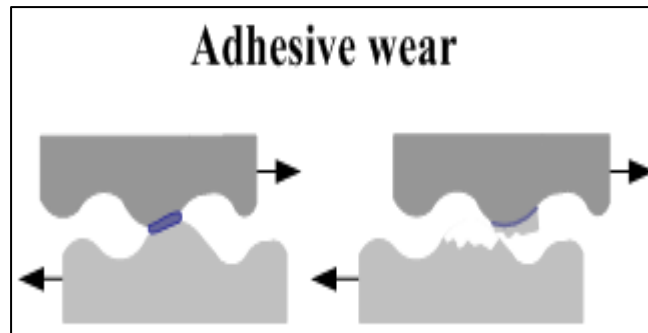
Figure 2. 5 Adhesive wear (Kopelivoich, 2012).

Past findings indicate that all forms of materials after cleaning can bond with other materials in vacuum to form strong connections. This is possible in view of the fact that the solubility of one material in another is likely to enhance adhesion which may influence friction rate or wearing to some levels lower than the melting points of the material in absolute units, (Montgomery, 1991). Moreover, empirical research on ceramic materials has not documented high adhesive bond strength partially because of the difficulty in finding equivalent lattice that match perfectly. Nevertheless, it has been observed that when different ceramics are rubbed on each other, there is an increased probability that some incidental and sufficient alignment of lattice occur to form strong adhesive bonding, (Kleis and Kulu, 2008). Figure2.6 elaborates on the mechanisms of adhesive wear.
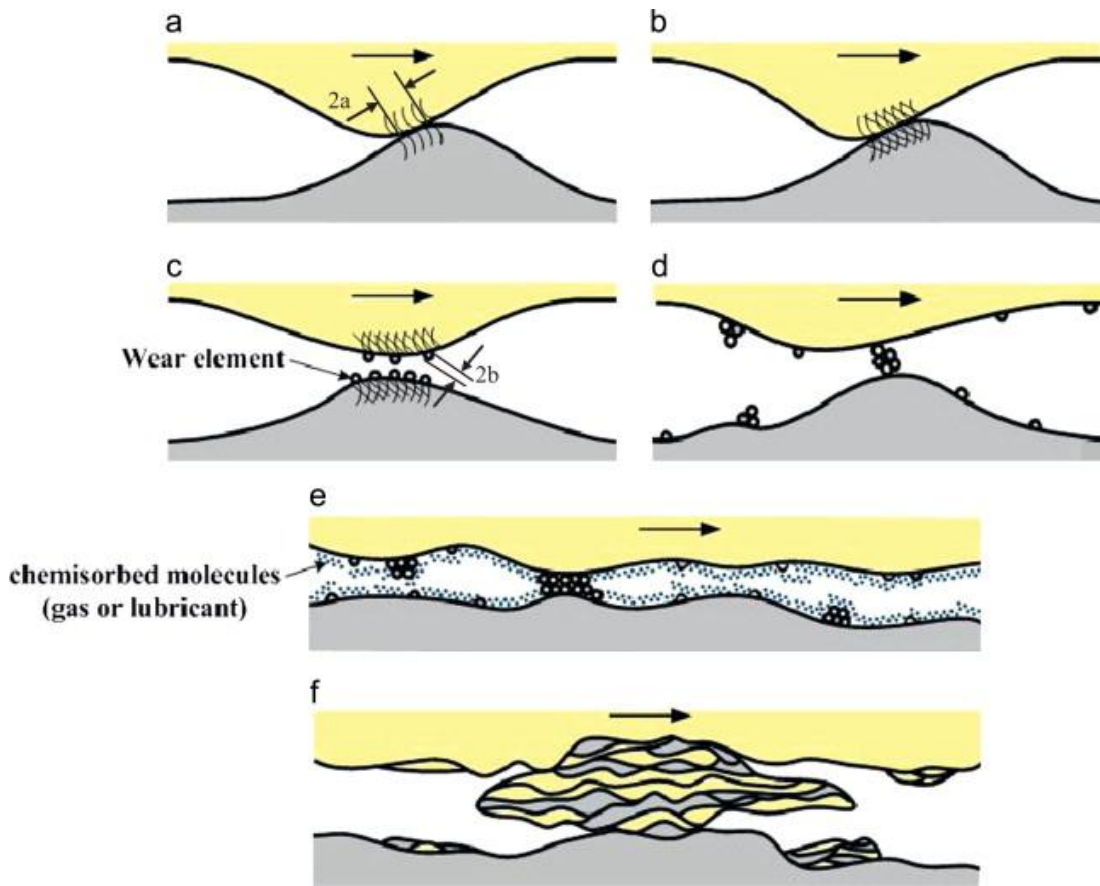
Figure 2. 6 Model of adhesive wear from the elementary process of generation of wear elements (a) to (c) to the formation of wear particles from (d)→(e) for mild wear, or (d)→(f) for severe wear. "*a*" and "*b*" in the figure mean a mean radius of each junction and each wear element, respectively(Mishina and Hase).

Alternatively, adhesive wearing has also been attributed to material transfer due to symbiotic relations or material overlap between relative movements by two bodies. The observation is mainly defined as plastic deformation of minute surface fragments within the superficial layers. The stringencies or microscopic wearing found on the surface of intermingling material helps to describe the severity on how

oxide fragments are pulled off and added to the surface of another material, partially as a result of strong adhesive forces between atomic structures or because of the accumulation in plastic energy zone between the asperities throughout the process of relative motion, (Rabinowicz and Mutis, 1965). The outcome of adhesive wear is largely linked to growing roughness and creation of lumps or protrusions on the original surface layer, and this outcome results in reaching of the oxidized layer on material surfaces, resulting to direct communication with underlying bulk material which may result in strong material bonding and increased plastic flow on the axial of the lump, (Brobakken and Zachrisson, 1981).

In order to understand how the wearing material flows, accelerates and is transported around the lump, trials are run to assess the nominal sliding velocity and the geometry which remain paramount in defining the contact pressure of the materials, and the emitted temperature during sliding, (Sınmazçelik and Taşkıran, 2007). Therefore, lumps on the surface contour are used to define the mathematical functions for the acceleration of the flowing material. As a result of these prerequisites, in remains explicit that the developed temperature and contact pressure rely largely on the geometry of the lumps ,(Jones and Scott, 1983). The table below indicates the friction and wear of sliding couples under experimental conditions in 50% air, 20 degrees centigrade and on a load of 10N.

Table 1 Friction and wear of sliding couples in 50% air, 20 degrees centigrade, and

10N load (Habig, 1990)

| Disk Lubricant Material | Film or Solid | Pin Material | Friction Coeff. | Disk Wear Rate $(mm^3/Nm \times 10^{-3})$ | Pin Wear Rate $(mm^3/Nm \times 10^{-3})$ |
|---|---|---|---|---|---|
| Polyphenylene Sulfide Composite | Solid | 440C | 0.30 | 6200 | 0 |
| Polyimide (PI-4701) | Film | 440C | 0.13 | 4000 | 0 |
| Poly(amide-imide) Composite | Solid | 440C | 0.37 | 1800 | 0 |
| Polyimide/Graphite Powder Composite | Solid | 440C | 0.37 | 900 | 0 |
| UHMWPE | Solid | 440C | 0.10 | 380 | 0 |
| Polyimide/Graphite Fiber Composite | Solid | 440C | 0.19 | 120 | 0 |
| Sputtered MoS$_2$ Vacuum | Film | 440C | 0.05 | 70 | 0 |
| Sputtered MoS$_2$ Air | Film | 440C | 0.07 | 64 | 0 |
| Polyimide (100°C) | Film | 440C | 0.02 | 8 | 0 |
| Diamond-like Carbon | Film | 440C | 0.05 | 2800 | 0.02 |
| PS-200 | Film | Cobalt Alloy | 0.28 | 2100 | 3000 |

The table above indicates the adhesive wear and friction various sliding material surface in contact illustrating that low wear and low friction do not always happen at the same time.  In traction drive low wear and high friction is often required and it should not be assumed that having high friction will lead to have high adhesive wear.

## 2.5 Summary of the literature

In statistics RSM is widely applied in defining a mathematical relationship between one or more variables and a response or multiple responses. In statistics, there is an important aspect of RSM where it is used as a statistical technique and as a mathematical approach to empirical model building. Through careful design models, it is possible to obtain efficient machinery sections with an efficient response (output variable) for example increased machinery efficiency and reduction in friction's drag force.

When optimizing machinery to reduce friction and adhesion between the interacting surfaces, an engineer may be compelled to search for the relationship between parameters that control the output of the system such as the applied force (x1) and the sliding velocity (x2) that usually accelerate the wearing rate (response y) of machine parts. The wearing of machines (response) as a function of the amount of applied force and sliding velocity (variables). Therefore, the interacting machinery planes where the wearing phenomenon is detected can be represented by the function $f$(x1, x2) which is its proportional or direct response surface. From the above, the importance of RSM can be clearly in term of engineering applications.

# CHAPTER 3

# METHODOLOGY

## 3.1 Material Selection and Experimental Procedure

Currently, there is considerable interest in using natural fibres as reinforcements in numerous applications. One of the best-known natural fibres is kenaf, which is traditionally grown for the production of twine, rope and sackcloth (Nishimura et al., 2012). In recent years there has been a high demand for, and interest in, the use of kenaf fibres for composites, due to their good mechanical properties. Kenaf fibre has thus found its way into industrial applications in a range of domains, including automotive, housing, packaging and electrical products(De Rosa et al., 2009). In the light of this, kenaf fibre was selected as the reinforcement in the current study.

Liquid epoxy (DER 331), a liquid reaction product of epichlorohydrin and disponol A, was used as the resin in this study. It is widely used for general purposes and is recognised as used in a standard form. It is suitable for applications such as casting and tooling, composites and automotive parts. The curing agent used for this epoxy was JOINTMINE 905-3S, a low viscosity aliphatic amine for room temperature curing. It has good wetting properties and impact resistance.

### 3.1.1 Kenaf Fiber Selection and Preparation

Raw kenaf fibres were supplied by the Malaysian Agricultural Research and Development Institute. The fibres had been well extracted, since they did not contain much dirt (**Figure 3.1a**). However, they were soaked in warm water for three hours until the fibres become yellow to indicate the cleaning process completed and then cleaned with fresh water. To extract the undesired substances, the fibres were combed and then dried for 24 hours in an oven at 40 $^{o}$C. The oven contained a fan to aid the drying process. A micrograph of the cleaned fibres is shown in **Figure 3.1b**. Other natural fibres have a waxy outer layer that covers their inner structure. This has been noted with oil palm (Ghali et al., 2011), coir (Saw et al., 2012), and banana fibres (Merlini et al., 2011). NaOH treatment was necessary to clean these natural fibres. For the current study, a preliminary investigation was performed to determine the interfacial adhesion of the fibre before treatment, which showed that kenaf fibres exhibit good interfacial adhesion with epoxy resin without treatment. Despite this, treatments were performed on a portion of the cleaned fibres and an evaluation of the interfacial adhesion and the tensile and flexural properties of the kenaf-epoxy composites were conducted with both treated and untreated fibres.
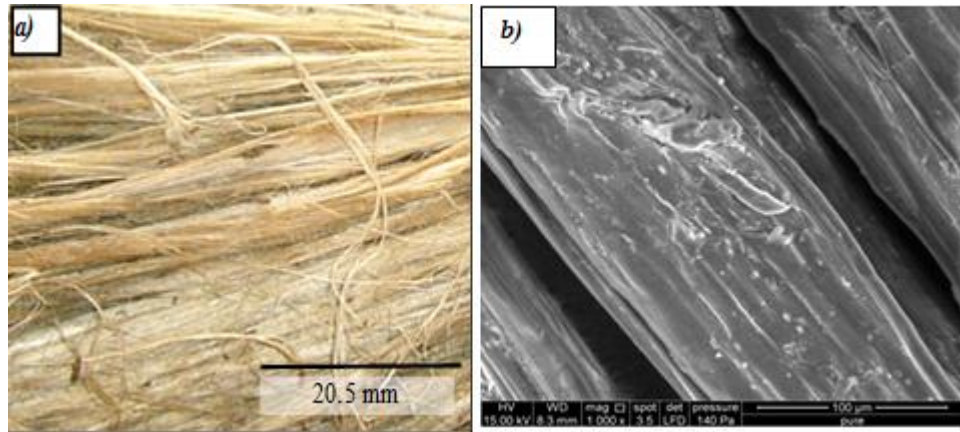
Figure 3. 1 Untreated kenaf fibres: (a) Photo of the raw fibre; (b) Micrograph of

cleaned fibres (Chin and Yousif, 2010).

In the treatment process, a portion of the cleaned kenaf fibres were cut into an average length of 100 mm. A NaOH solution was prepared with a 6 weight per cent concentration. The selected fibres were immersed in this aqueous NaOH solution for 24 hours at room temperature. After treatment, the fibres were washed with tap water and then dried for 24 hours in an oven at a temperature of 40 $^{\circ}$C.

Samples of the micrographs of the treated kenaf fibres are shown in **Figure 3.2**. Comparing **Figure 3.1b** and **Figure 3.2**, it was evident that the NaOH treatment had thoroughly cleaned the surfaces of the fibres, the inner bundles of the fibres were exposed and any undesired substances had been removed. This may result in better interfacial adhesion of the kenaf fibres and the epoxy matrix, a hypothesis that was tested and will be discussed in Section 3.3.
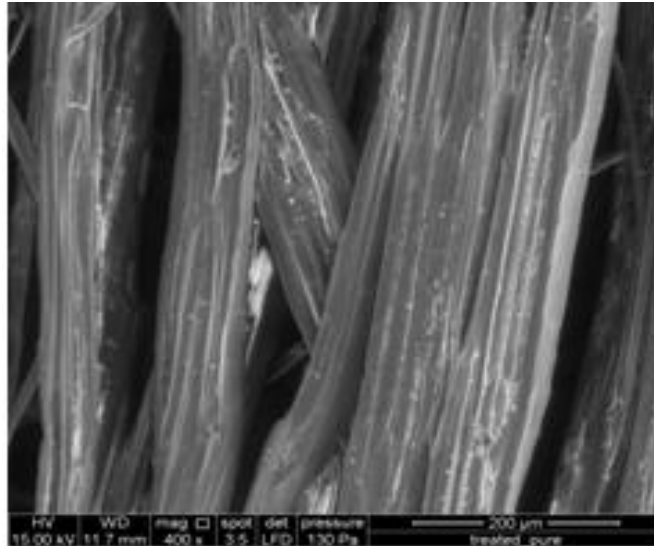
Figure 3. 2 Micrographs of the treated kenaf fibres(Chin and Yousif, 2010).

### 3.1.2 Epoxy Composite Preparation

The fabrication process was the same for the mechanical and tribological samples, except for the dimension of the sample, which was controlled by the mould used in the fabrication process. The epoxy resin and the hardener were uniformly mixed at a 2:1 ratio using an electric stirrer and then poured into the desired mould. The mould was placed in a vacuum chamber (MCP 004PLC) at a pressure of 0.5 bar to remove any air bubbles trapped in between the fibres. The vacuum extracted blocks were kept for curing at room temperature for 24 hours. The volume fraction of the fibre in the matrix was controlled to be approximately 48 per cent vol. A sample of the prepared composite is shown in **Figure 3.3, a–c**. Comparing **Figure 3.3 b** and **c** clearly shows that the NaOH treatment enhanced the bonding regions of the fibre with the matrix.
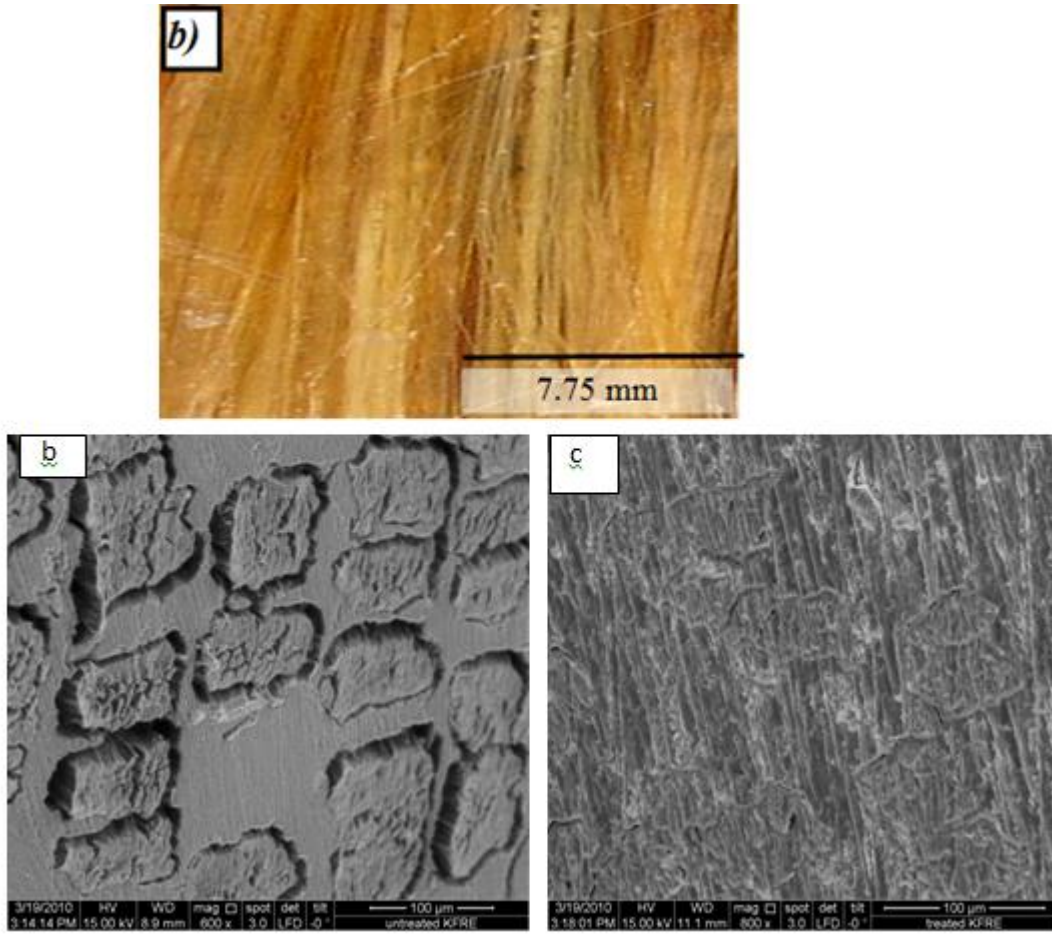
Figure 3. 3 SEM micrographs of cross-sections of KFRE composites: a) Photo of the composite; b) Untreated kenaf fibre; c) Treated kenaf fibres (Chin and Yousif, 2009)

## 3.2 Experimental Procedure

A BOD machine was used for these experiments, and is shown in **Figure 3.11**. The composite surface specimens (10 mm × 10 mm × 20 mm) were rubbed against a stainless steel (AISI 304, hardness=1,250 HB, Ra=0.1 μm) counterface under dry/wet contact conditions. For intimate contact between the specimen and the stainless steel counterface, the specimen's contact surface was polished by abrasive

paper (Sic G2000) and then cleaned with a dry soft brush. The roughness of the composite surface varied in each orientation. In the parallel and anti-parallel orientations, the average roughness of five measurements in different regions was around 0.30 μm (**Figure 3.12a**). Meanwhile, in the N-O, the composite roughness values were an average of approximately 0.70 μm (**Figure 3.12b**).
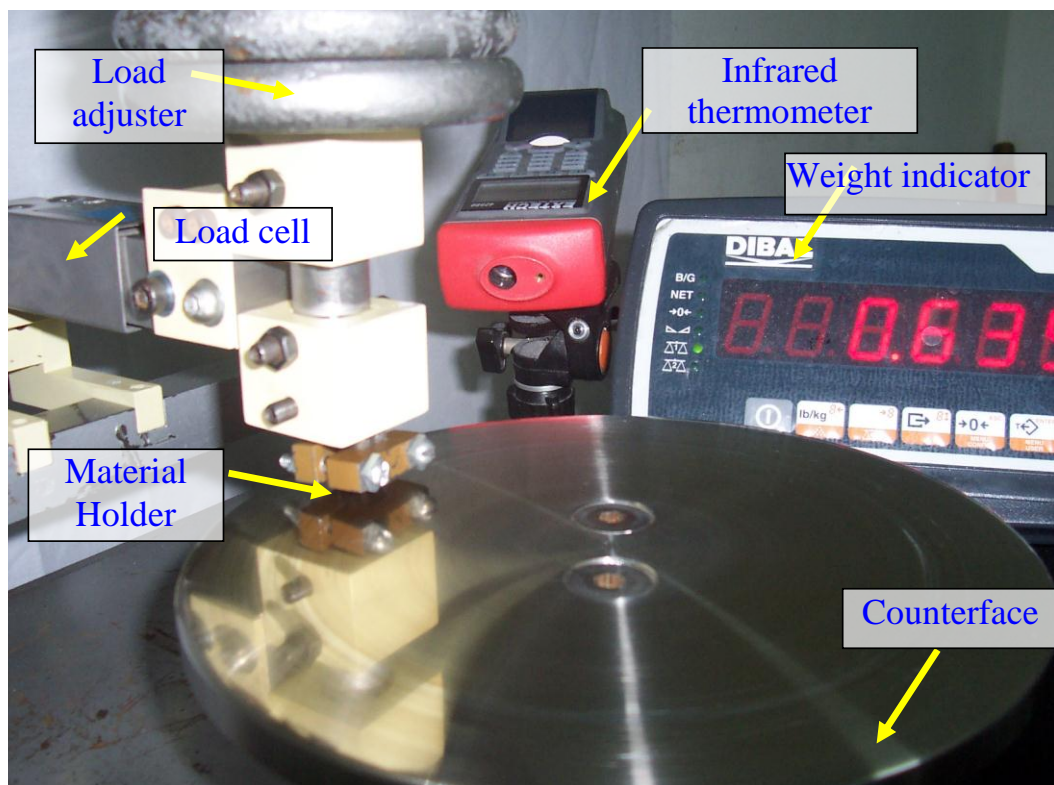


Figure 3. 4 the BOD machine working under dry contact conditions (Yousif, 2013, Chin and Yousif, 2009)

Before and after the test, the specimens were dried in an oven at 40 $^o$C for 12 hours. A Setra balance (±0.1 mg) was used to determine the weights of the specimens. The

specific wear rate (Ws) at each operating condition was determined using the following equation:

$$Ws = \frac{\Delta W / \rho}{L \times D}$$

Where:

Ws: Specific wear rate (mm$^3$/Nm)

$\Delta W$: Weight loss (mg)

$p$: Density (kg/m$^3$)

$L$: Applied load (N)

$D$: Sliding distance (m)

During the tests, frictional force was measured by a load cell, which was fixed at the middle of the lever that applied the loads.

For the wet adhesive wear test, tap water was supplied to the interface via a pump with flow rate of 0.2 l/min. After each test, the worn surface was coated with a thin layer of gold using an ion sputtering device (JEOL, JFC-1600) and a scanning electron microscope (JEOL, JSM 840) was used to observe the surface. Each tribological test was repeated three times and the average of the measurements were determined.

During the dry adhesive wear tests, an infrared thermometer (Extech 42580) was used to measure the initial interface temperature and calibration was performed to determine the interface temperature. In the calibration process, the infrared thermometer was pointed at the midpoint of interface between the specimen and the stainless steel counterface during the tests. The calibration of the temperature was carried out under stationary conditions. The counterface was heated using an external heat source. While the counterface was heated, a thermocouple was placed between the specimen and the counterface. The temperatures measured by both thermometers (infrared and thermocouple) were recorded simultaneously until the interface temperature reached approximately 80 C$^o$. This process was repeated three times and the averages were determined. The measured temperatures (thermocouple) were plotted against each other and the fit line was determined using the calibration equation.

## 3.3 Collected frictional data:

The credibility of data is very essential for the experiment to produce a highly reliable result that can be trusted and can be relied on. Collecting data can fall into two main categories, which are quantitative and qualitative research methods. The procedure, which was used to collect data in this report, was the quantitative method of collecting data. The quantitative research method usually calculate the information based on a random structure data collection that caverns different

experiences into a well-defined response categories which result in a set of data that is easy to compare, summarize and generalize (Creswell and Clark, 2007).

### 3.3.1 Machine used to conduct tribology test

The tribology machine was used to conduct a tribology test on a sample of Kenaf fibre which was brought from a Malaysian agriculture to measure the temperature and the friction coefficient for different applied loads and with variety of different speeds. Below is a table showing the produced excel sheet from the tribology machine at a speed of 2.8m/s.

Table 2 collected data from tribology machine when speed was set at 2.8 m/s

| 2.8m/s | | | | | | | | |
|---|---|---|---|---|---|---|---|---|
| | | | Friction | | | | Temperature | |
| Time | SD | 30 | 50 | 70 | 100 | 30 | 50 | 70 | 100 |
| 0 | 0 | 0 | 0 | 0 | 0.00 | 24 | 23 | 23 | 24.00 |
| 0.5 | 0.084 | 0.92 | 0.9 | 0.85 | 0.98 | 24 | 24 | 24 | 25.00 |
| 1 | 0.168 | 0.85 | 0.91 | 0.8 | 0.94 | 24 | 24.5 | 24 | 25.00 |
| 1.5 | 0.252 | 0.81 | 0.85 | 0.79 | 0.90 | 24.5 | 25 | 25 | 26.00 |
| 2 | 0.336 | 0.78 | 0.81 | 0.78 | 0.87 | 25 | 25 | 26 | 27.00 |
| 2.5 | 0.42 | 0.77 | 0.82 | 0.78 | 0.87 | 26 | 26 | 26 | 27.00 |
| 3 | 0.504 | 0.74 | 0.8 | 0.77 | 0.85 | 26.5 | 26 | 26 | 28.00 |
| 3.5 | 0.588 | 0.75 | 0.8 | 0.76 | 0.85 | 27 | 27 | 27 | 28.00 |
| 4 | 0.672 | 0.72 | 0.78 | 0.77 | 0.83 | 27.5 | 27 | 27 | 28.00 |
| 4.5 | 0.756 | 0.71 | 0.76 | 0.78 | 0.83 | 28 | 27 | 27 | 29.00 |
| 5 | 0.84 | 0.67 | 0.73 | 0.78 | 0.80 | 28 | 28 | 28 | 29.00 |
| 5.5 | 0.924 | 0.65 | 0.72 | 0.77 | 0.78 | 29 | 28 | 29 | 30.00 |
| 6 | 1.008 | 0.67 | 0.72 | 0.78 | 0.80 | 29 | 29 | 30 | 31.00 |
| 6.5 | 1.092 | 0.63 | 0.7 | 0.76 | 0.77 | 30 | 29 | 30 | 31.00 |
| 7 | 1.176 | 0.61 | 0.71 | 0.78 | 0.77 | 31 | 29 | 31 | 31.00 |
| 7.5 | 1.26 | 0.64 | 0.72 | 0.76 | 0.78 | 31 | 30 | 32 | 32.00 |
| 8 | 1.344 | 0.6 | 0.7 | 0.75 | 0.75 | 32 | 30 | 32 | 32.00 |
| 8.5 | 1.428 | 0.59 | 0.69 | 0.75 | 0.74 | 32 | 31 | 33 | 34.00 |
| 9 | 1.512 | 0.6 | 0.7 | 0.73 | 0.74 | 32 | 31.5 | 34 | 35.00 |
| 9.5 | 1.596 | 0.58 | 0.67 | 0.72 | 0.72 | 32 | 32 | 34 | 35.00 |
| 10 | 1.68 | 0.55 | 0.65 | 0.71 | 0.70 | 32.5 | 32 | 35 | 35.00 |
| 10.5 | 1.764 | 0.53 | 0.65 | 0.72 | 0.70 | 33 | 32 | 35 | 36.00 |
| 11 | 1.848 | 0.55 | 0.65 | 0.68 | 0.69 | 34 | 32 | 35 | 36.00 |
| 11.5 | 1.932 | 0.52 | 0.62 | 0.69 | 0.67 | 34.5 | 33 | 36 | 36.00 |
| 12 | 2.016 | 0.52 | 0.63 | 0.68 | 0.67 | 35 | 34 | 36 | 37.00 |
| 12.5 | 2.1 | 0.53 | 0.62 | 0.69 | 0.67 | 35 | 35 | 36 | 37.00 |
| 13 | 2.184 | 0.51 | 0.6 | 0.68 | 0.66 | 35.5 | 35 | 36 | 38.00 |
| 13.5 | 2.268 | 0.5 | 0.61 | 0.69 | 0.66 | 36 | 35 | 37 | 39.00 |
| 14 | 2.352 | 0.49 | 0.6 | 0.68 | 0.65 | 36.5 | 36 | 38 | 39.00 |
| 14.5 | 2.436 | 0.49 | 0.6 | 0.68 | 0.65 | 36.5 | 37 | 39 | 40.00 |
| 15 | 2.52 | 0.5 | 0.59 | 0.68 | 0.65 | 37 | 37 | 39 | 40.00 |
| 15.5 | 2.604 | 0.48 | 0.59 | 0.67 | 0.64 | 37 | 38 | 40 | 42.00 |
| 16 | 2.688 | 0.46 | 0.58 | 0.68 | 0.63 | 37.5 | 39 | 40 | 42.00 |
| 16.5 | 2.772 | 0.45 | 0.57 | 0.66 | 0.62 | 38 | 40 | 41 | 43.00 |

The above sample table is showing the data that was collected from the tribology machine. The first column on the left is representing the time in sec that is relative to the recoded data for the temperature and friction. The second column is showing the sliding distance in Km and it measures the data up to a distance of 5 Km. the $3^{rd}, 4^{th}, 5^{th}$ and $6^{th}$ column is showing the friction at different applied loads. In the $3^{rd}$ column the applied load is 30 N and in the $4^{th}$ column the applied load is 50 N. the applied load in the $5^{th}$ column is 70 N and in the $6^{th}$ column the applied load is 100 N. the $7^{th}$ column is representing the materials temperature at a load of 30 N where on the $8^{th}$ column the temperature is shown at a load of 50 N. the $9^{th}$ column represents the temperature at an applied load of 70 N and in the $10^{th}$ column the temperature is shown at an applied load of 100 N.

Table 3 is showing the data for a rotating speed of 1.1m/s and 3.1m/s.

**1.1m/s**

| Time | SD | Friction 50 | Temperature 50 |
|---|---|---|---|
| 0 | 0 | 0 | 22 |
| 0.5 | 0.084 | 0.35 | 23 |
| 1 | 0.168 | 0.91 | 23 |
| 1.5 | 0.252 | 0.85 | 24 |
| 2 | 0.336 | 0.8 | 23 |
| 2.5 | 0.42 | 0.78 | 24 |
| 3 | 0.504 | 0.79 | 23 |
| 3.5 | 0.588 | 0.8 | 24 |
| 4 | 0.672 | 0.85 | 25 |
| 4.5 | 0.756 | 0.79 | 25 |
| 5 | 0.84 | 0.78 | 26 |
| 5.5 | 0.924 | 0.77 | 26 |
| 6 | 1.008 | 0.77 | 25 |
| 6.5 | 1.092 | 0.76 | 26 |
| 7 | 1.176 | 0.75 | 26 |
| 7.5 | 1.26 | 0.75 | 26 |
| 8 | 1.344 | 0.74 | 27 |
| 8.5 | 1.428 | 0.73 | 27 |
| 9 | 1.512 | 0.75 | 27 |
| 9.5 | 1.596 | 0.75 | 28 |
| 10 | 1.68 | 0.77 | 28 |
| 10.5 | 1.764 | 0.76 | 29 |
| 11 | 1.848 | 0.74 | 29 |
| 11.5 | 1.932 | 0.75 | 29 |
| 12 | 2.016 | 0.76 | 30 |
| 12.5 | 2.1 | 0.77 | 30 |
| 13 | 2.184 | 0.74 | 30 |
| 13.5 | 2.268 | 0.74 | 30.5 |
| 14 | 2.352 | 0.74 | 31 |
| 14.5 | 2.436 | 0.75 | 31 |
| 15 | 2.52 | 0.76 | 31.5 |
| 15.5 | 2.604 | 0.74 | 32 |
| 16 | 2.688 | 0.74 | 32 |
| 16.5 | 2.772 | 0.74 | 33 |
| 17 | 2.856 | 0.75 | 33 |
| 17.5 | 2.94 | 0.73 | 33 |
| 18 | 3.024 | 0.74 | 34 |
| 18.5 | 3.108 | 0.7 | 34 |
| 19 | 3.192 | 0.72 | 35 |
| 19.5 | 3.276 | 0.73 | 35 |
| 20 | 3.36 | 0.71 | 36 |
| 20.5 | 3.444 | 0.72 | 36 |

**3.1m/s**

| Time | SD | Friction 50 | Temperature 50 |
|---|---|---|---|
| 0 | 0 | 0 | 23 |
| 0.5 | 0.084 | 0.935 | 24 |
| 1 | 0.168 | 0.88 | 25 |
| 1.5 | 0.252 | 0.83 | 26 |
| 2 | 0.336 | 0.79 | 27 |
| 2.5 | 0.42 | 0.775 | 28 |
| 3 | 0.504 | 0.765 | 30 |
| 3.5 | 0.588 | 0.775 | 32 |
| 4 | 0.672 | 0.785 | 33 |
| 4.5 | 0.756 | 0.75 | 34 |
| 5 | 0.84 | 0.725 | 36 |
| 5.5 | 0.924 | 0.71 | 37 |
| 6 | 1.008 | 0.72 | 38 |
| 6.5 | 1.092 | 0.695 | 40 |
| 7 | 1.176 | 0.68 | 42 |
| 7.5 | 1.26 | 0.695 | 43 |
| 8 | 1.344 | 0.67 | 45 |
| 8.5 | 1.428 | 0.66 | 47 |
| 9 | 1.512 | 0.675 | 48 |
| 9.5 | 1.596 | 0.665 | 50 |
| 10 | 1.68 | 0.66 | 51 |
| 10.5 | 1.764 | 0.645 | 52 |
| 11 | 1.848 | 0.645 | 53 |
| 11.5 | 1.932 | 0.635 | 54 |
| 12 | 2.016 | 0.64 | 55 |
| 12.5 | 2.1 | 0.65 | 56 |
| 13 | 2.184 | 0.625 | 57 |
| 13.5 | 2.268 | 0.62 | 58 |
| 14 | 2.352 | 0.615 | 60 |
| 14.5 | 2.436 | 0.62 | 61 |
| 15 | 2.52 | 0.63 | 62 |
| 15.5 | 2.604 | 0.61 | 63 |
| 16 | 2.688 | 0.6 | 64 |
| 16.5 | 2.772 | 0.535 | 65 |
| 17 | 2.856 | 0.605 | 66 |
| 17.5 | 2.94 | 0.575 | 67 |
| 18 | 3.024 | 0.53 | 68 |
| 18.5 | 3.108 | 0.56 | 69 |
| 19 | 3.192 | 0.565 | 70 |
| 19.5 | 3.276 | 0.565 | 71 |
| 20 | 3.36 | 0.56 | 72 |
| 20.5 | 3.444 | 0.57 | 72 |

The above table is another example of the excel sheet that was produced by the tribology machine and it is showing the conducted tribology test results for the Kenaf fibre. The test was conducted according to these speeds (1.1m/s and 3.1m/s); the first column on the left is again showing the time in (sec). On the second column from the left the (SD) column is representing the sliding distance for the rotor which is rotating up to a distance of 5 Km. the third column represents the friction coefficient at an applied load of 50N and the fourth column represents the corresponding temperature at a load of 50 N in degrees Celsius.

## 3.4 Software used to analyse the data:

There is a long variety and a wide range of different statistical software in today's world; as a result it was challenging to choose the software that would be used to do the analysis of the data. After a long time of research and a recommendation of the supervisor Minitab statistical software was chosen to be the program to perform all the statistical analysis needed because of its simplicity and its ease of use. Minitab is very powerful statistical software that is able to do all the statistical analysis needed for this study. On figure 4.5 below is a screenshot showing the layout of the Minitab program. Minitab is mainly consists of two windows an upper window and the down window, the upper window is called the session window and its purpose to show the result of the analysed statistical data also it shows the commands or tasks that Minitab was asked to perform. The down window is the worksheet window which is a spread sheet where the data is inputted and it can be easily manipulated. In the worksheet window the inputted data can be inputted as a text, numerical or date and this depends on the type of data that the experimenter has. The data can be entered manually in the worksheet or it can be copied and pasted directly from an excel spread sheet. Many different designs of experiments (DOE) can be conducted using Minitab program such as factorial, response surface, mixture and taguchi. The main objective for using the response surface methodology in this research paper is for modelling and predicting purposes.
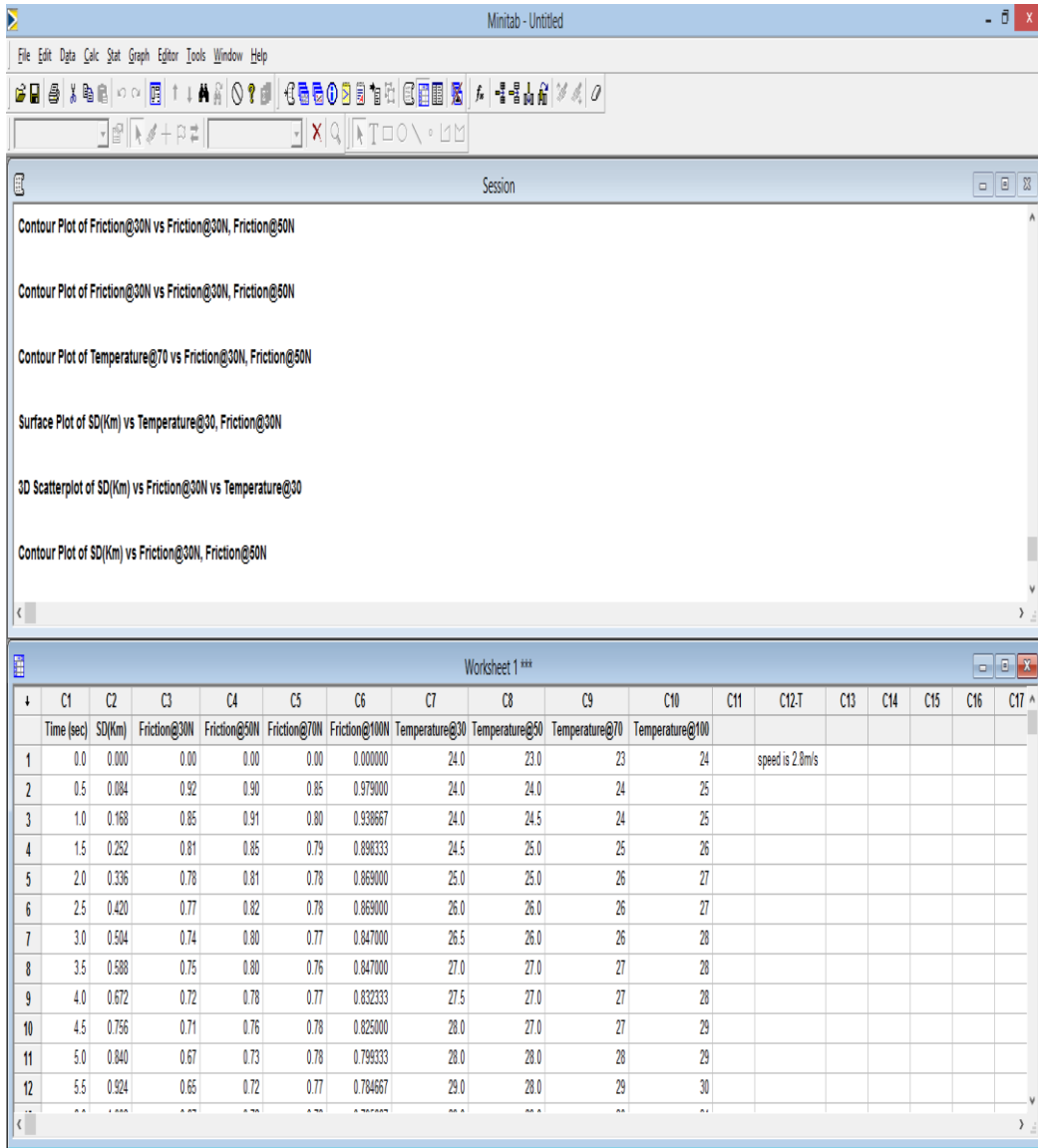
Figure 3. 5 screenshot showing the Minitab software

# CHAPTER 4

# RESULT AND DISCUSSION

## 4.1 Dry Adhesive Frictional Behaviour of Composites

The frictional force was captured during each experiment for all operating parameters. Due to the large volume of data collected, it was summarised and is presented in this section. The friction coefficients versus the sliding distances at different applied loads and velocities for the NE and the KFRE composites were developed and a sample of the frictional data is given in **Figure 4.4**. The figure displays the friction coefficient against the sliding distance for the KFRE composite at N-O under different applied loads at a sliding velocity of 2.8 m/s. All materials showed similar frictional behaviour at all the operating parameters tested; i.e., the frictional coefficient was high at the start of the sliding (running-in) and then reached a steady state after a sliding distance of approximately 4 km. This behaviour is common in both natural fibre-polymer and synthetic fibre-polymer composites, since there is a high shear force in the contact zone in the first stage of the adoption process between the asperities in contact. After this stage, a steady state friction coefficient is achieved if there is no change in the contacted surfaces. For synthetic fibre-polymer composites, stability of the friction coefficient has been reported in studies of carbon-epoxy(Zhou et al., 2009), glass or a carbon-aramid hybrid weave-epoxy and three-dimensional braided carbon fibre-epoxy (Ahmed and Vijayaragan, 2006). The instability of the friction coefficient of the synthetic fibre-polymer

composites is mainly due to the modifications that occur on the track surface of the
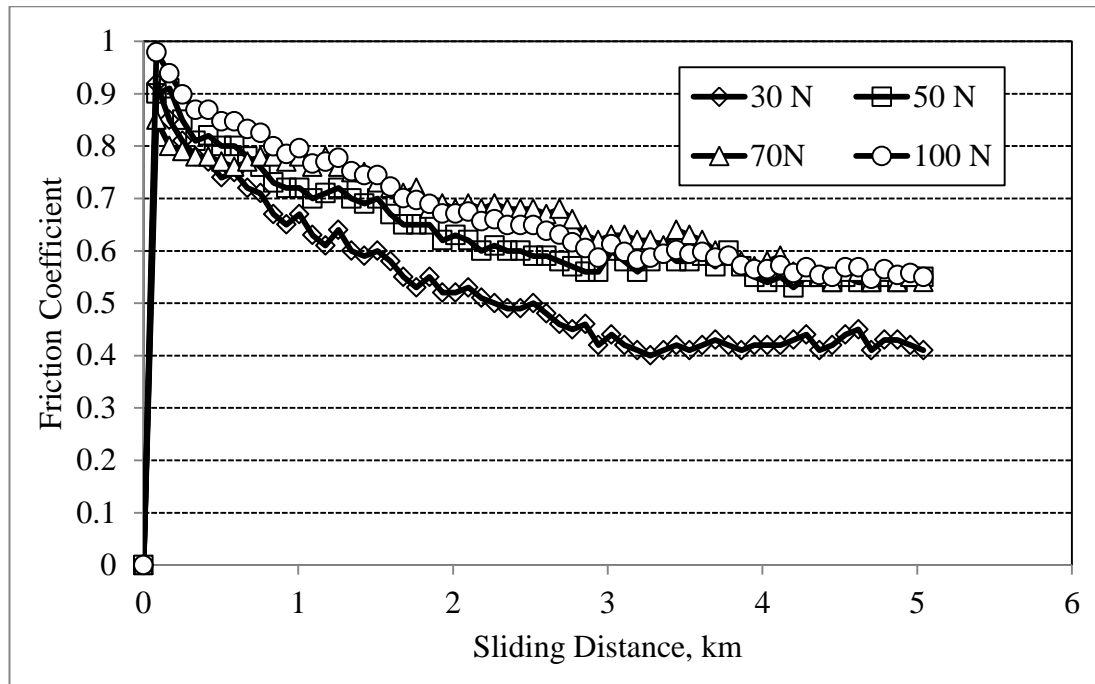counterface (Salih et al., 2013).



Figure 4. 1 Sample of the frictional data showing the coefficient versus sliding

distance of KFRE in N-O at a sliding velocity of 2.8 m/s.

To examine the influence of the applied load on the friction coefficient and frictional

behaviour of the composites, the average of the friction coefficient after a 5 km

sliding distance was determined for all materials under different applied loads and is

presented in **Figure 4.5**. NE and KFRE in N-O exhibited higher friction coefficients

(0.5–0.75) than the other composites. KFRE in AP-O exhibited a relatively low

friction coefficient (0.32–0.42). From the wear behaviour (see Section 4.2.1), the

wear resistance in the KFRE composite in N-O is higher than that of other composites, which indicates high resistance at the interface and reflects the high friction coefficient at this fibre orientation. In the case of the NE, the wear property was much lower than its composites and hence the frictional behaviour of NE is relatively poor compared to its composites. It appears that the film transfer on the counterface has high adhesion characteristics, which causes stickiness between the asperities and leads to a high friction coefficient. This is followed by detachment of the film, resulting in high levels of material removal. This is illustrated in **Figure 4.6** and will be discussed further in a later section.
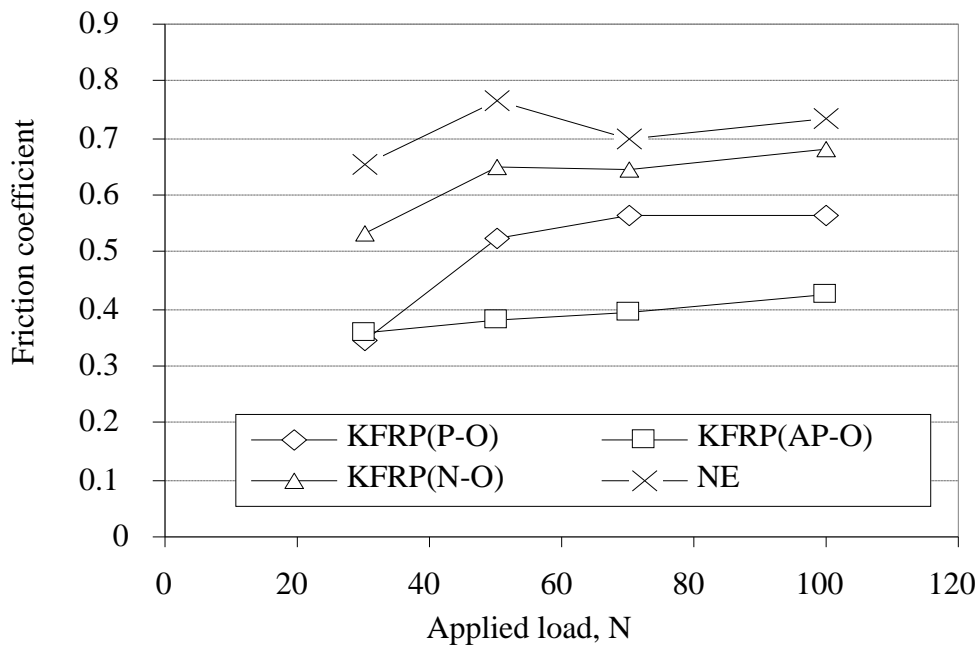


Figure 4. 2 Friction coefficient versus applied load for NE and KFRE at different

orientations.

As a result of dry sliding, heat is generated at the interface, which can play an important factor in determining the wear mechanism of the materials. **Figure 4.7**

delineates the maximum interface temperature that was measured during the rubbing at the longest sliding distance of 5 km at different applied loads. Due to the high friction coefficient of the NE and the KFRE composite in N-O, higher interface temperatures were produced compared to KFRE composites in P-O and AP-O. Despite the high interface temperatures, the maximum temperature did not reach the $T_g$ of the epoxy (approximately 125 $C^o$). However, the presence of the heat associated with the shear loading at the interface may combine with the load at the interface to become thermo-mechanical and then cause deterioration of the soft surface. A plastic deformation and/or softening process may be expected to take place in the resinous regions of the composites during sliding.
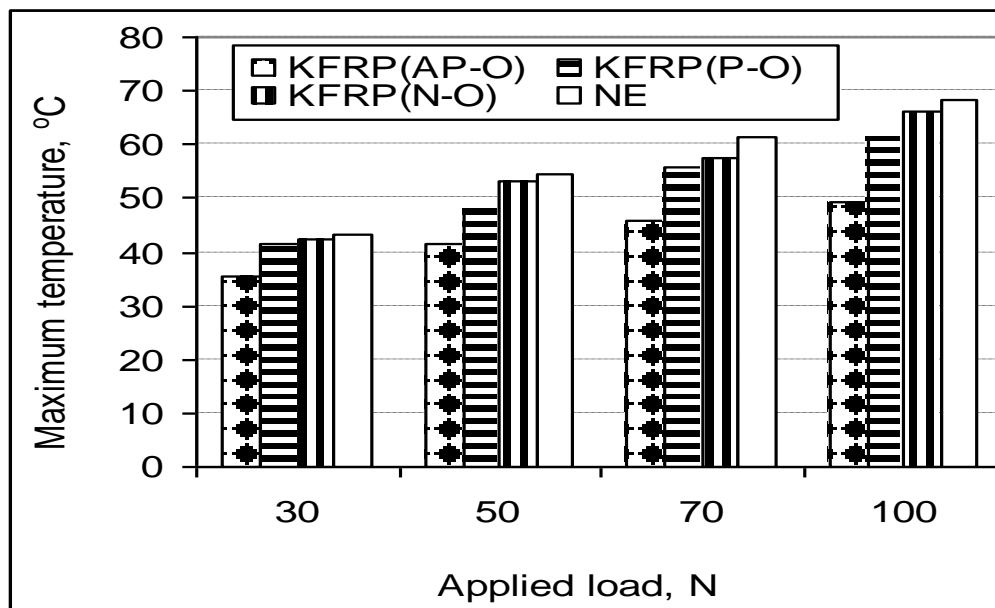


Figure 4. 3 Interface temperatures versus applied load

4.2 **Effects of applied loads on friction**.

The test of the Kenaf fiber sample was conducted using different applied loads. The first experiment was conducted with an applied load of 30N then the load was increased to 50N. Furthermore, the experiment was performed for a load of 70N and lastly for a load of 100 N.  The figures below are showing the Sliding distance plotted against friction for different applied loads, and the results will be compared between the different applied loads to see the effect of increasing or changing the applied load.
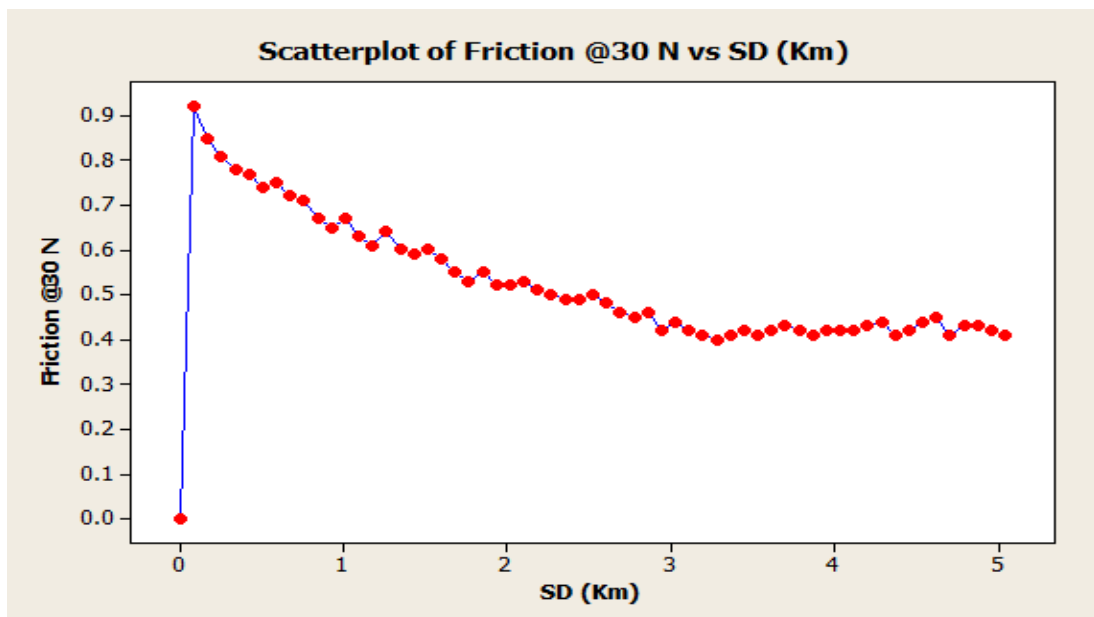


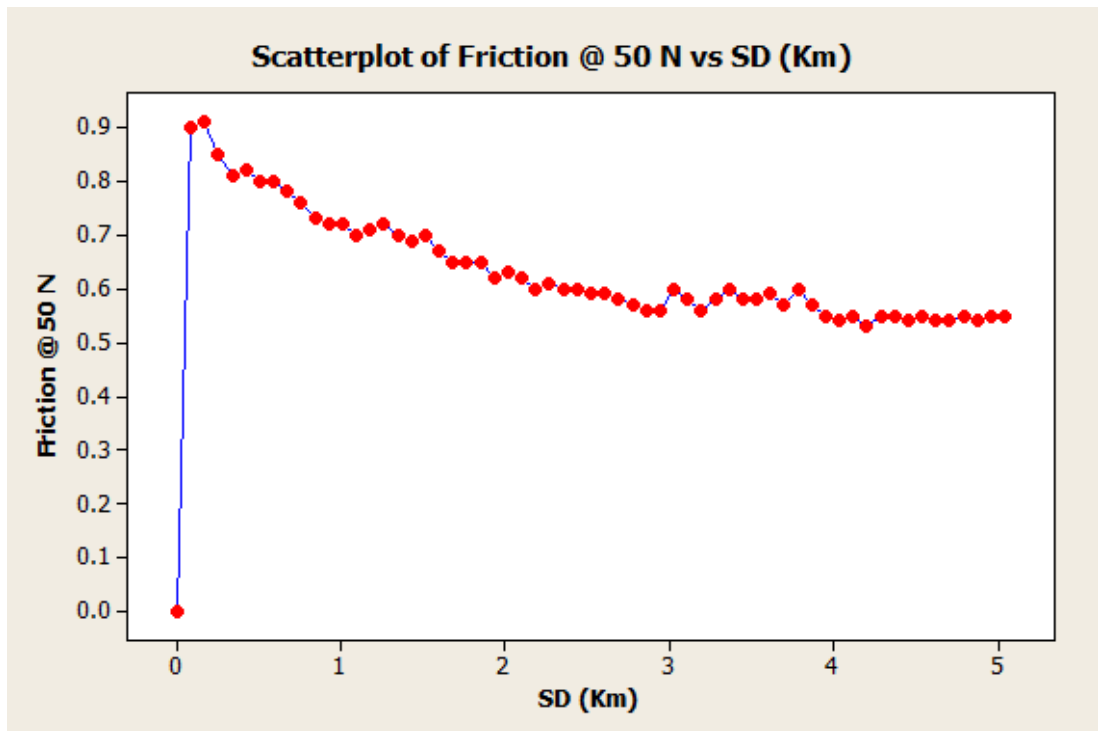Figure 4. 4 Friction @ 30 N verses Sliding Distance (Km)

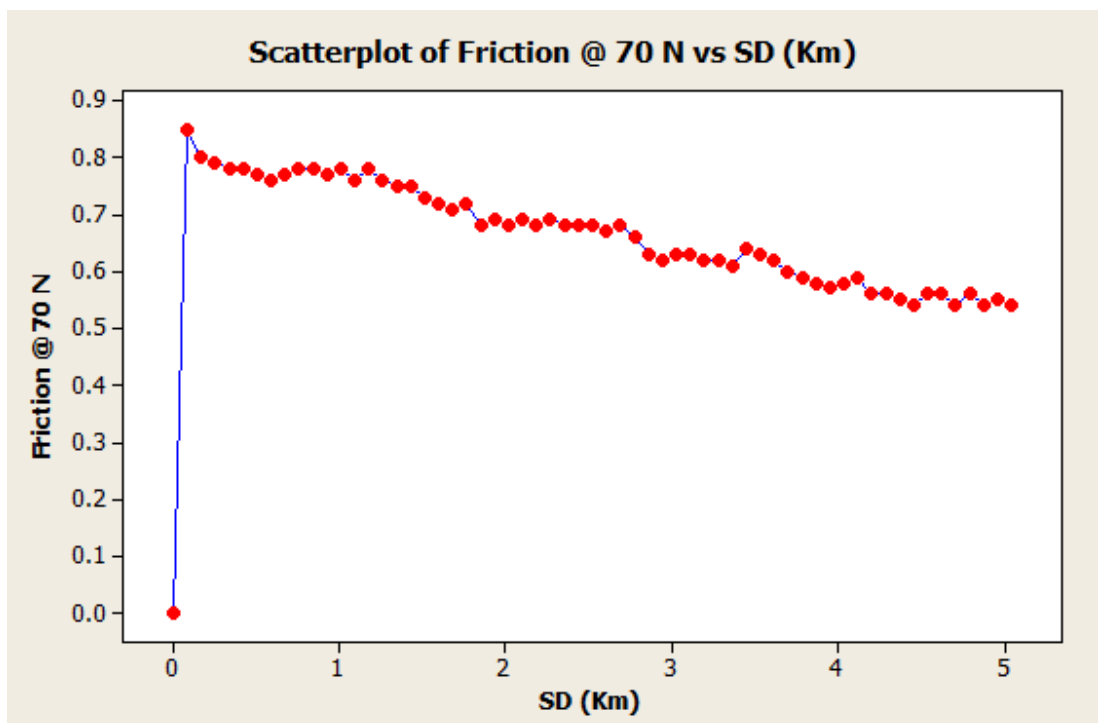Figure 4. 5 Friction @ 50 N verses Sliding Distance (Km)



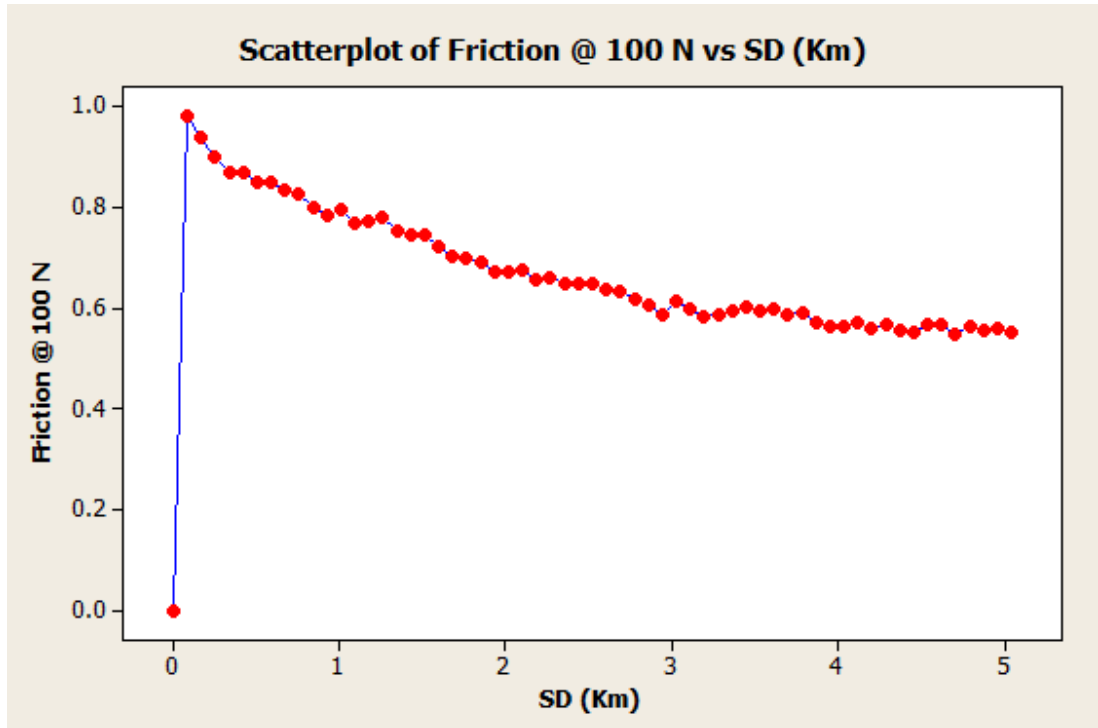Figure 4. 6 Friction @ 70 N verses Sliding Distance (Km)

Figure 4. 7 Friction @ 100 N verses Sliding Distance (Km)

Generally the effect of increasing the applied load can be explained as, it has a proportional effect on increasing the friction coefficient. On other words when the load increases the friction coefficient increases as well. On fig (4.4) the friction coefficient starts at about 0.92 and then it was rapidly decreasing until it reaches 2.5 Km sliding distance then the line has flatten out and start to slowly slide until it reaches 3.5 Km at a friction coefficient of nearly 0.45 after that the line starts to oscillate from 0.4 and 0.5 until it reaches the final sliding distance of 5 Km and 0.41 frictional coefficient. Fig (4.5) shows the sliding distance verses friction at an applied load of 50 N. the friction coefficient initially starts at 0.9 and the heavily drooped until it reaches 0.5 at a sliding distance of about 3 Km. after sliding distance

of 3 Km the friction line starts oscillating until it was at 4.2 Km sliding distance then the friction coefficient start slowly increasing until it stops at 0.55 friction coefficient. Fig (4.6) shows the sliding distance verses friction at 70N applied load. The friction coefficient starts at about 0.86 then it was slightly declining until about 0.5 Km sliding distance the it was slowly increasing until 1.1 Km then again it was gradually falling until it reaches sliding distance of 2.2 Km. the friction coefficient continued descending slowly until it came to stationary at friction coefficient of about 0.54. Lastly on fig (4.7) is the sliding distance verses friction at an applied load of 100N. The friction coefficient start at a value of 0.98 and at first it had a heavy drop until it reaches 0.79 at a sliding distance of 1.2 Km then the friction coefficient line slowly was decreasing until it reaches 0.58 at a sliding distance of 3.2 Km where the friction coefficient line level off until it stops at a friction value of 0.55. From all the above it can be concluded that, the load has a direct effect on the friction value. When the load increases it produces more friction on the Kenaf fibre sample because it pushes the rotor disk more tightly on the Kenaf sample and thus the value of friction increases when the applied load increases.

**4.3 Effects of different applied loads on temperature.**

As it is widely known wherever there is friction there will be temperature as well. Also whenever, the value of friction increases temperature value increases as well(Bijwe, 1997). In this section, a study of the effect of different applied loads on

temperature will be conducted and discussed. The following graphs show the behaviour of temperature at different applied loads.
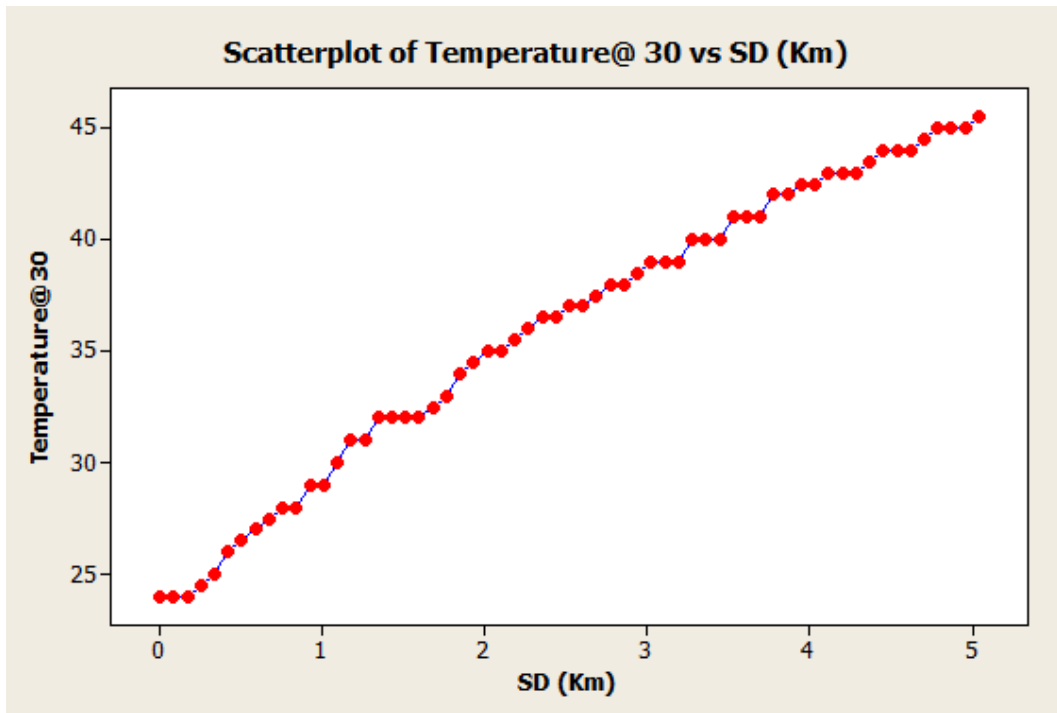


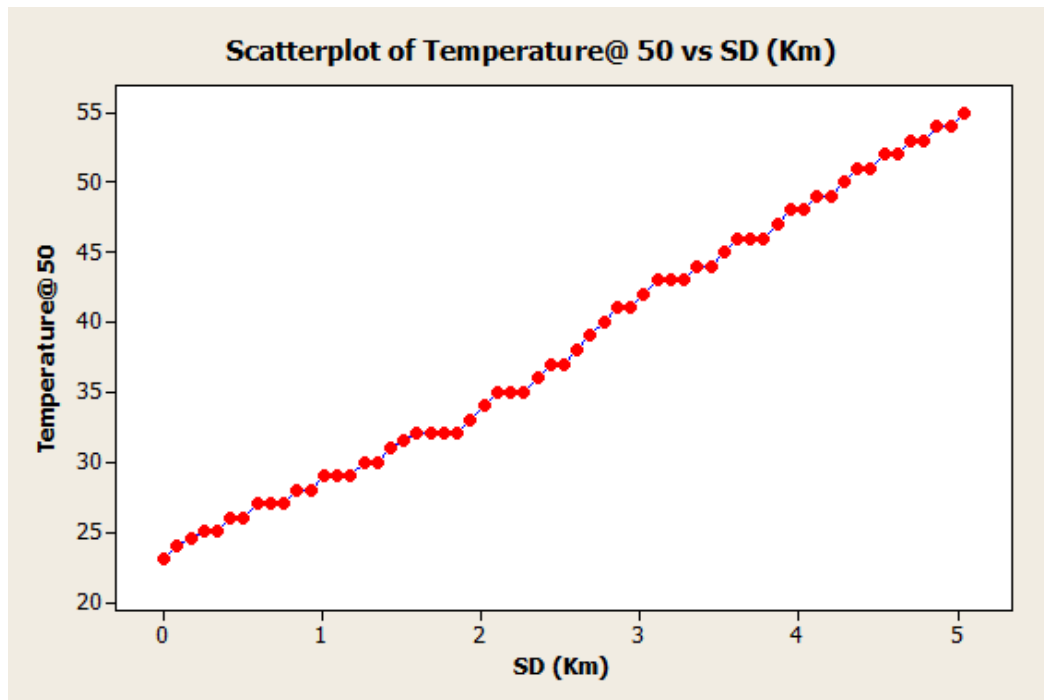Figure 4. 8 Temperature @ 30 N verses Sliding Distance (Km)

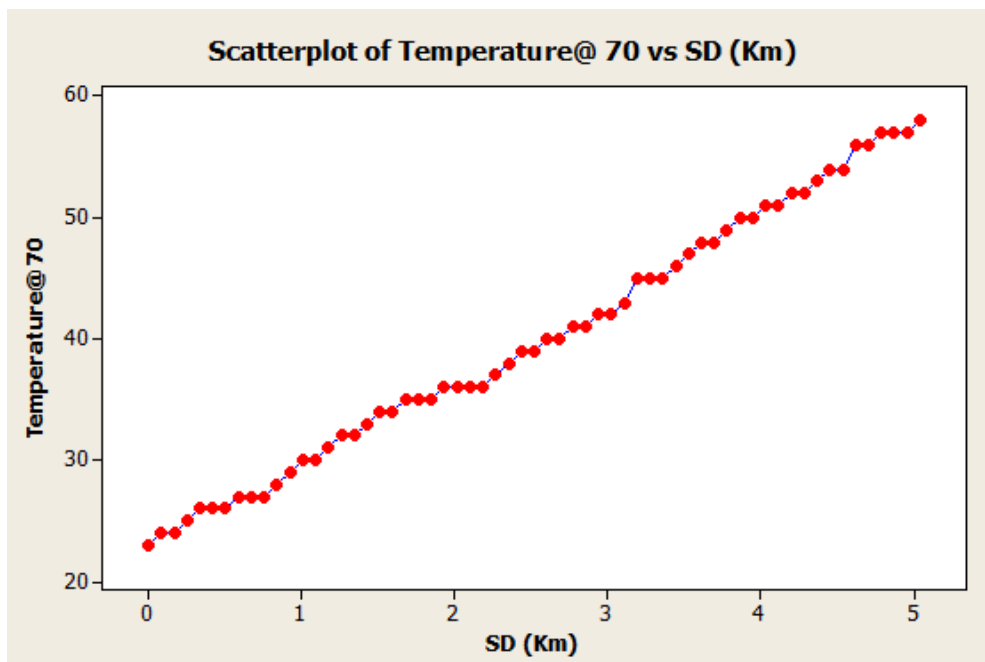Figure 4. 9 Temperature @ 50 N verses Sliding Distance (Km)



Figure 4. 10 Temperature @ 70 N verses Sliding Distance (Km)
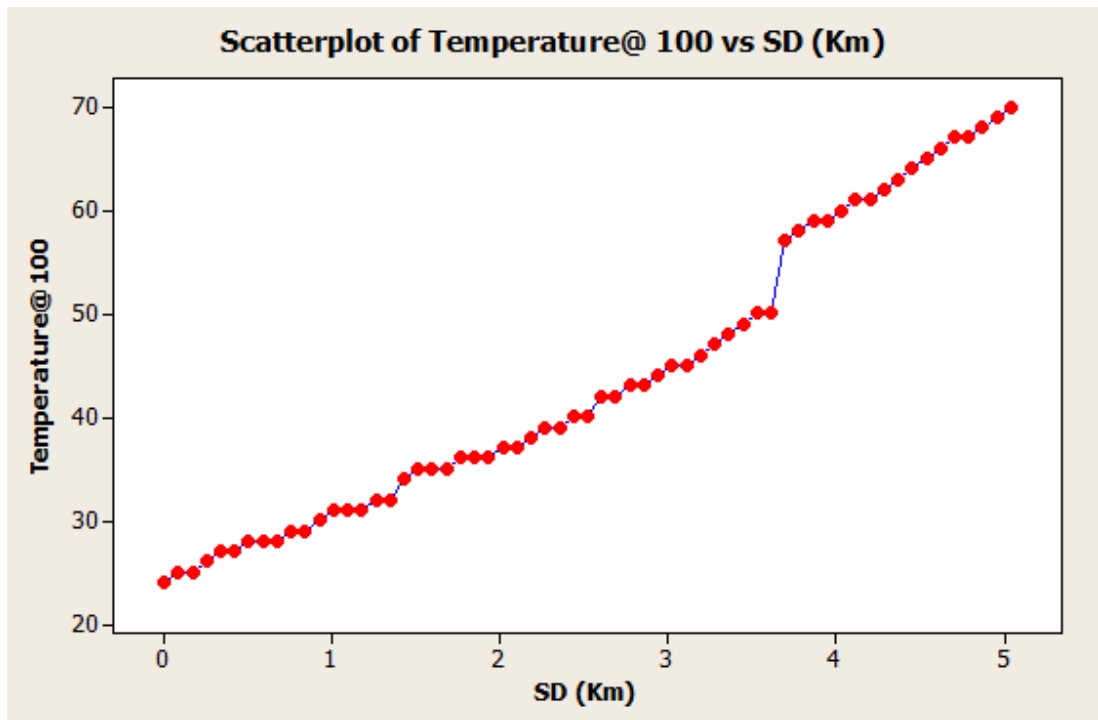
Figure 4. 11 Temperature @ 100 N verses Sliding Distance (Km)

In fig (4.8) where temperature is plotted verses sliding distance at an applied load of 30 N, it can be noticed that, the temperature starts at about 24 Co and the temperature line was held steady until it reaches 0.16 Km sliding distance then temperature increases rapidly until it reaches 33 Co then temperature levelled off and continued going steady until it reaches 1.8 Km. after that the temperature starts rising until it reaches 45.5 Co. fig (4.9) is showing the temperature at an applied load of 50 N verses the sliding distance. The temperature starts at about 23 $C^o$ then gradually it was increasing until it reaches 32 $C^o$ at a sliding distance of 1.8 Km then the temperature line has flatten out until it reaches sliding distance of 2 Km the it was steadily climbing until it reaches a value of 55 $C^o$. in fig (4.10) is the temperature at

an applied load of 70 N plotted against the sliding distance. At the start temperature was 23 C$^o$ then the temperature was slightly increasing until it comes to 26 C$^o$ at a sliding distance of 0.86 Km it levelled off until it reaches 1 Km sliding distance then it starts climbing again until it reaches 36 C$^o$ at a sliding distance of 1.8 Km then the temperature stabilised until sliding distance of 2.2 Km then the temperature was steadily rising until it reaches 58 C$^o$. finally in fig (4.11) is the temperature at an applied load of 100N plotted against the sliding distance. The temperature starts at 24 C$^o$ then it was steadily increasing until 1.4 Km sliding distance then it had a rapid increasing where it reaches 34 C$^o$ then it was gradually increasing again until it reaches 50 C$^o$. after the temperature reaches 50 C$^o$ at about 3.6 Km sliding distance there was a rapid rising again from 50 to 60 C$^o$ the temperature was steadily increasing until it reaches a final value of 70 C$^o$. from all the above it can be concluded that load differences is a key factor in changing the temperature. When the load increases the temperature value increases as well, due to the increment of the friction factor and this has a direct effect on the temperature.

**4.4 Effect of rotating speed on friction**

As it was mentioned earlier, the conducted tribology test was done for four different rotating speeds. The test was conducted at running speed of 1.1m/s, 2.8m/s, 3.1m/s and 3.5m/s. in the following we will investigate the effect of changing the rotating speed on friction and temperature. The below graph is illustrating the behaviour of friction at rotating speeds of 1.1m/s and 2.8m/s.

Figure 4. 12 Friction coefficient at rotating speeds of 1.1m/s and 2.8m/s verses time

From the above figure, generally it can be said that the friction coefficient decreases when the rotating speed increases as it can be clearly seen from the figure. At time 0.5 sec the rotating speed of 1.1m/s had a higher friction coefficient than the rotating speed of 2.8 m/s then they all start decreasing. After 4 seconds of time had pass the rotating speed of 1.1 m/s start to get higher readings for friction than the founded readings for friction at rotating speed 2.8m/s. The gap between the two different rotating speeds starts to widen up after passing 11 sec where the friction coefficient for the rotating speed of 1.1m/s was 0.74 and the friction coefficient for the rotating speed of 2.8 m/s was 0.65. The test ended at time 30 sec and the final reading for friction at the rotating speed of 1.1 m/s was 0.7 and the final friction reading at the rotating speed of 2.8 m/s was 0.55.
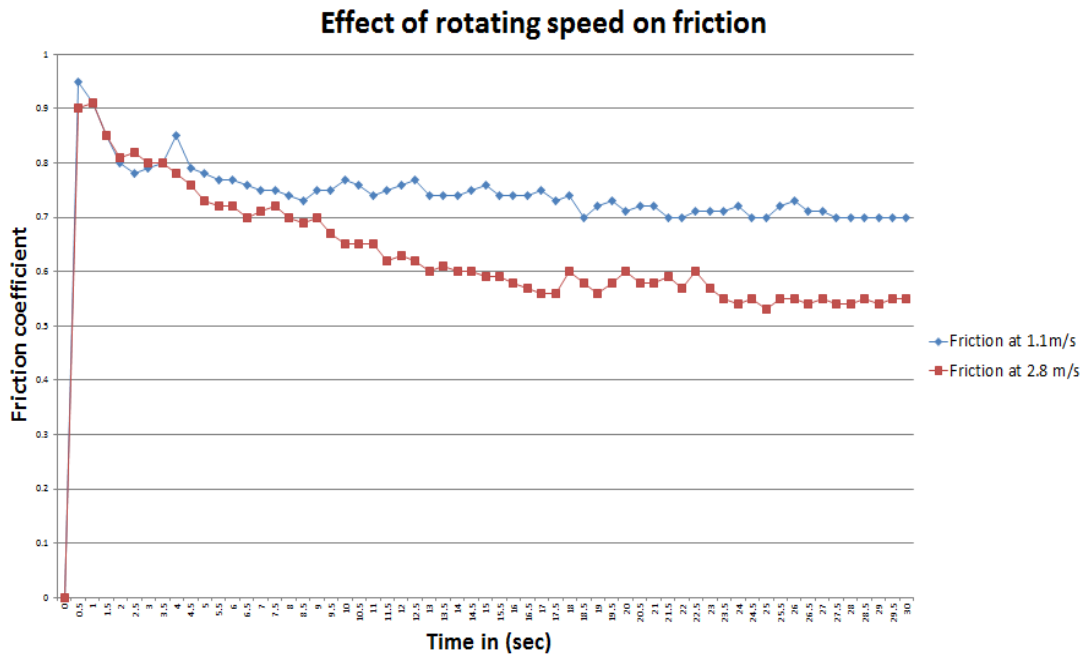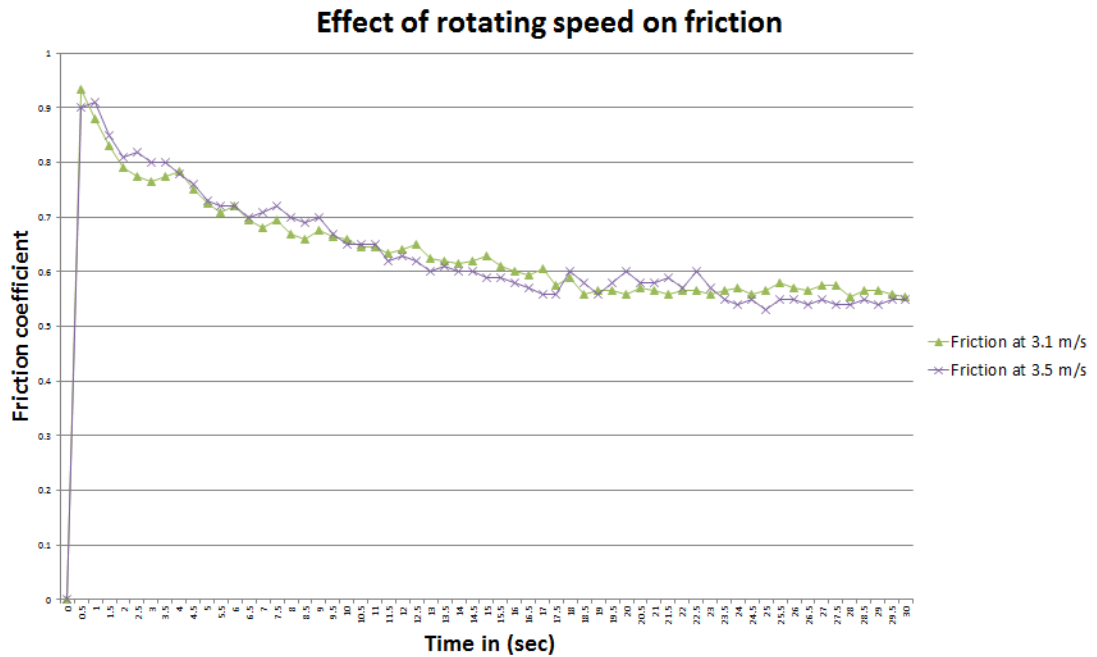
Figure 4. 13 Friction coefficient at rotating speeds of 3.1m/s and 3.5m/s verses time

From the above figure it can be clearly seen that the difference between the friction coefficients for the two rotating speeds (3.1m/s & 3.5m/s) does not have a noticeable change, which is might be the cause of not making a big difference between the two rotating speeds. At the start and at a time of 1 sec the two frictional coefficients were almost at the same point then they start varying a little bit up and downs until they reach the end of the experiment with the same friction coefficient readings.

The table below is illustrating the change in friction coefficient for the different rotating speeds and it is also showing the decrease in percentage relative to the first and final friction coefficient.

Table 4 Comparison between friction coefficients at different rotating speeds

| Rotating speed (m/s) | First friction coefficient at time 0.5 sec | final friction coefficient at time 30 sec | Change in percentage (%) |
|---|---|---|---|
| 1.1 | 0.95 | 0.7 | 30.303 |
| 2.8 | 0.9 | 0.55 | 48.2759 |
| 3.1 | 0.935 | 0.55 | 51.8519 |
| 3.5 | 0.9 | 0.55 | 48.2759 |

From table 4.1 it can be noticed that, the percentage change in friction coefficient increase when the rotating speed increases however, this is not the case when comparing the rotating speed of 2.8m/s and 3.5m/s which had the same percentage of change as well as the same readings for friction with respect to time.

## 4.5 Effect of rotating speed on temperature

The speed of the rotter has a tremendous effect on determining the temperature of the Kenaf fibre. The temperature increase dramatically with the increment of the rotating speed, because when the rotating speed increases the interaction between the kenaf fibre and the rotter increases as well, which in turn produces more friction and heat. The following figure is showing the behaviour of temperature with different rotating speeds.
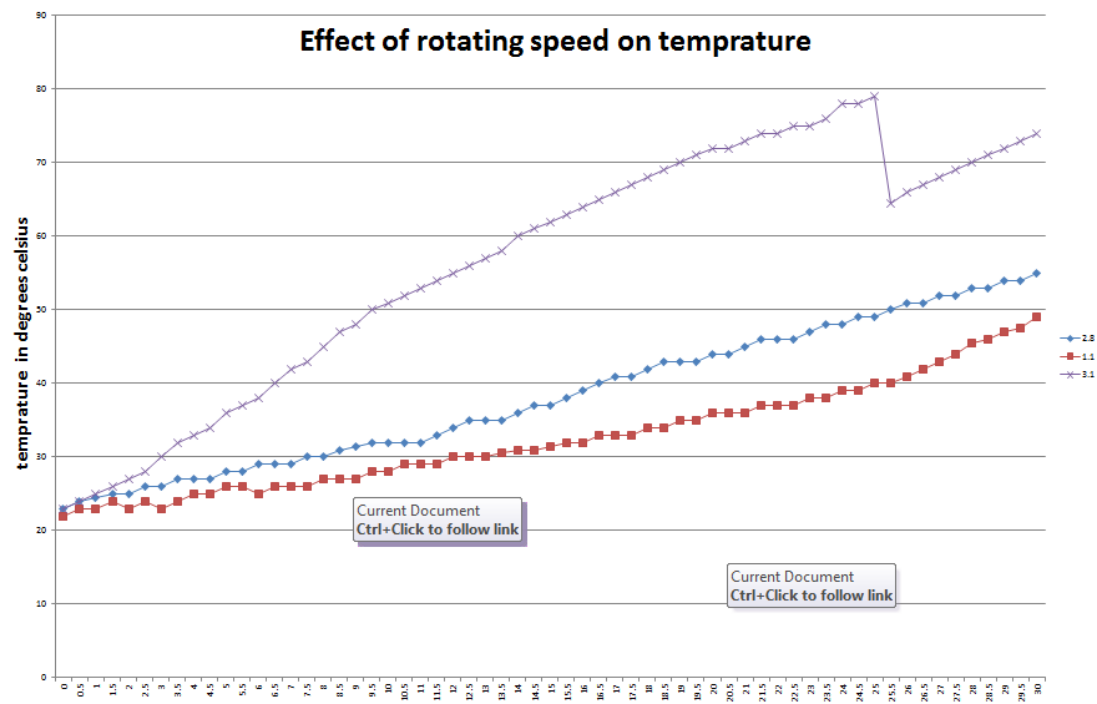


Figure 4. 14 temperature verses time for different rotating speeds

It can be clearly seen from the above graph that the temperature increases when the rotating speed increases. The kenaf fibre samples were all at room temperature at the start of the experiment and their temperatures were at about 22-23 Co. At rotating speed of 1.1m/s the increment of temperature was slowly increasing until it reaches 49 Co, the relationship of the rotating speed at 1.1m/s and temperature was linearly described with an $R^2$ value of 0.9637 and the relationship is $y = 0.3975x + 20.267$. Temperature scores higher values with the rotating speed of 2.8m/s, the temperature at the end of the test was 55 Co and the relationship between the temperature and the rotating speed 2.8m/s was linearly described by the following relation $y = 0.5396x + 21.585$ and the value of $R^2$ was 0.9934 which means that, the accuracy is very high. On the other hand, the relationship between temperature and rotating speed at of 3.1m/s could not be described linearly because it had very low value of R2 so, it was necessary to increase the order of the polynomial to meet an accurate result and the relation was described by a second degree polynomial which is $y = 0.019x^2 + 2.0691x + 16.618$.

# Chapter 5

## Conclusion

In conclusion, response surface methodology is a mathematical approach that is very useful for optimization and predicting purposes. According to results obtained in chapter 4 the following is concluded:

- Frictional behaviour of composites has a high frictional coefficient at the begging of the tribology test because of the high shear force in the contact zone.

- Friction coefficient and temperature increases when the applied load is increased.
- The rotating speed has a direct effect on temperature so that temperature increases when rotating speed increases. Temperature will increase 5 Co for every 0.1 m/s increment in the rotating speed.

Friction coefficient decreases with the increment of the rotating speed.

Furthermore, empirical equations representing temperature and friction for the Kenaf fibre composite were predicted for different situations with respect to time (x):

Table 5 the derived empirical equations

| Load (N) | Speed (m/s) | Temperature Equations | Friction equations |
|---|---|---|---|
| 50 | 1.1 | Temperature $= 0.0042x^2 + 0.139x + 22.982$ | Friction$= -0.05928-0.06411 \log(x)$ |
| 50 | 2.8 | Temperature $= 0.5396x + 21.585$ | Friction$= -0.03386-0.1567\log(x)$ |
| 50 | 3.1 | Temperature $= -0.0006x^3 + 0.0394x^2 + 0.4211x + 26.922$ | Friction$= -0.04768-0.1419\log(x)$ |

# References

AHMED, K. S. & VIJAYARAGAN, S. 2006. Elastic property evaluation of jute-glass fibre hybrid composite using experimental and CLT approach. *INDIAN JOURNAL OF ENGINEERING AND MATERIALS SCIENCES,* 13**,** 435.

BATIST, R. D. 1972. *Internal friction of structural defects in crystalline solids*, Amsterdam.

BHUSHAN, B. Tribology and mechanics of magnetic storage devices, 1996. Springer-Verlag, New York.

BHUSHAN, B. 2001. *Fundamentals of tribology and bridging the gap between the macro- and micro/nanoscales*, Springer.

BHUSHAN, B. & GUPTA, B. K. 1991. Handbook of tribology: materials, coatings, and surface treatments.

BIGONI, D. 2012. *Nonlinear Solid Mechanics: Introduction; 2. Elements of tensor algebra and analysis; 3. Solid mechanics at finite strains; 4. Isotropic nonlinear hyperelasticity; 5. Solutions of simple problems in finitely deformed nonlinear elastic solids; 6. Constitutive equations and anisotropic elasticity; 7. Yield functions with emphasis on pressure-sensitivity; 8. Elastoplastic constitutive equations; 9. Moving discontinuities and boundary value problems; 10. Global conditions of uniqueness and stability; 11. Local conditions for uniqueness and stability; 12. Bifurcation of elastic solids deformed incrementally; 13. Applications of local and global uniqueness and stability criteria to non-associative elastoplasticity; 14. Wave propagation, stability and bifurcation; 15. Post-critical behaviour and multiple shear band formation; 16. A perturbative approach to material instability*, Cambridge University Press.

BIJWE, J. 1997. Composites as friction materials: Recent developments in non-asbestos fiber reinforced friction materials—a review. *Polymer composites,* 18**,** 378-396.

BOX, G. E. & DRAPER, N. R. 2007. *Response surfaces, mixtures, and ridge analyses*, Wiley-Interscience.

BROBAKKEN, B. O. & ZACHRISSON, B. U. 1981. Abrasive wear of bonding adhesives: studies during treatment and after bracket removal. *American journal of orthodontics,* 79**,** 134-147.

CHIN, C. W. & YOUSIF, B. F. 2010. Tribological behaviour of KFRE composite. *International Journal of Modern Physics B,* 24**,** 5589-5599.

COLES, J. M., CHANG, D. P. & ZAUSCHER, S. 2010. Molecular mechanisms of aqueous boundary lubrication by mucinous glycoproteins. *Current Opinion in Colloid & Interface Science,* 15**,** 406-416.

COOK, B. A., HARRINGA, J. L., ANDEREGG, J., RUSSELL, A. M., QU, J., BLAU, P. J., HIGDON, C. & ELMOURSI, A. A. 2010. Analysis of wear mechanisms in low-friction AlMgB<sub> 14</sub>—TiB<sub> 2</sub> coatings. *Surface and Coatings Technology,* 205**,** 2296-2301.

CORNELL, J. A. 2011. *Experiments with mixtures: designs, models, and the analysis of mixture data*, Wiley.

CRESWELL, J. W. & CLARK, V. L. P. 2007. *Designing and conducting mixed methods research*, Wiley Online Library.

DANIEL, I. M., ISHAI, O., DANIEL, I. M. & DANIEL, I. 1994. *Engineering mechanics of composite materials*, Oxford university press New York.

DE ROSA, I. M., SANTULLI, C. & SARASINI, F. 2009. Acoustic emission for monitoring the mechanical behaviour of natural fibre composites: A literature review. *Composites Part A: Applied Science and Manufacturing,* 40**,** 1456-1469.

DE SAXCÉ, G. & FENG, Z.-Q. 1998. The bipotential method: a constructive approach to design the complete contact law with friction and improved numerical algorithms. *Mathematical and Computer Modelling,* 28**,** 225-245.

DEGARMO, R., GIBSON, S. & BALVANZ, L. 2003. Method and apparatus for processing wet material. Google Patents.

DINIZ, F. M. & MARTIN, A. M. 1996. Use of response surface methodology to describe the combined effects of pH, temperature and E/S ratio on the hydrolysis of dogfish (Squalus acanthias) muscle. *International journal of food science & technology,* 31**,** 419-426.

GHALI, L. H., ALOUI, M., ZIDI, M., DALY, H. B., MSAHLI, S. & SAKLI, F. 2011. Effect of chemical modification of luffa cylindrica fibers on the mechanical and hygrothermal behaviours of polyester/luffa composites. *BioResources,* 6**,** 3836-3849.

GOYAL, S., RUINA, A. & PAPADOPOULOS, J. 1991. Planar sliding with dry friction part 1. limit surface and moment function. *Wear,* 143**,** 307-330.

HABIG, K.-H. 1990. Friction and wear of sliding couples coated with TiC, TiN or TiB< sub> 2</sub>. *Surface and Coatings Technology,* 42**,** 133-147.

HOLMBERG, K., MATTHEWS, A. & RONKAINEN, H. 1998. Coatings tribology—contact mechanisms and surface design. *Tribology International,* 31**,** 107-120.

HOYT, J. 1972. A Freeman Scholar Lecture: The Effect of Additives on Fluid Friction. *Journal of Basic Engineering,* 94**,** 258.

JIN, Z., DOWSON, D. & FISHER, J. 1997. Analysis of fluid film lubrication in artificial hip joint replacements with surfaces of high elastic modulus. *Proceedings of the Institution of Mechanical Engineers, Part H: Journal of Engineering in Medicine,* 211**,** 247-256.

JONES, M. H. & SCOTT, D. 1983. *Industrial Tribology: The Practical Aspects of Friction, Lubrication and Wear*, North Holland.

KHURI, A. I. & MUKHOPADHYAY, S. 2010. Response surface methodology. *Wiley Interdisciplinary Reviews: Computational Statistics,* 2**,** 128-149.

KLEIS, I. & KULU, P. 2008. *Solid particle erosion: occurrence, prediction and control*, Springer.

KOPELIVOICH. 2012. *Mechanisms of wear* [Online]. SubsTech. Available: http://www.substech.com/dokuwiki/doku.php?id=mechanisms_of_wear [Accessed 16 Sep 2013].

KUHN, M., GOLD, P. & LOOS, J. 2003. Wear protection and low friction in roller bearings by different PVD-coating systems. *Tribology Series,* 43**,** 459-465.

LARSON, R. & FARBER, B. 2006. *Elementary statistics*, Pearson Custom Pub.

LIN, J. F. & CHOU, C. C. 2002. The response surface method and the analysis of mild oxidational wear. *Tribology International,* 35**,** 771-785.

LUCAS, J. M. 1994. How to achieve a robust process using response surface methodology. *Journal of Quality Technology,* 26**,** 248-260.

MAJUMDAR, A. & BHUSHAN, B. 1990. role of fractal geometry in roughness characterization and contact mechnaics of surfaces. *Journal of Tribology,* 112**,** 205-216.

MERLINI, C., SOLDI, V. & BARRA, G. M. 2011. Influence of fiber surface treatment and length on physico-chemical properties of short random banana fiber-reinforced castor oil polyurethane composites. *Polymer Testing,* 30**,** 833-840.

MISHINA, H. & HASE, A. Wear equation for adhesive wear established through elementary process of wear. *Wear*.

MONTGOMERY, D. C. 1991. *Introduction to statistical quality control*, Wiley New York.

MYERS, R. H. & ANDERSON-COOK, C. M. 2009. *Response surface methodology: process and product optimization using designed experiments*, John Wiley & Sons.

NISHIMURA, A., KATAYAMA, H., KAWAHARA, Y. & SUGIMURA, Y. 2012. Characterization of kenaf phloem fibers in relation to stem growth. *Industrial Crops and Products,* 37**,** 547-552.

OEHLERT, G. 2000a. Design and analysis of experiments. WH Freeman and Company, New York.

OEHLERT, G. W. 2000b. *A first course in design and analysis of experiments*, WH Freeman New York.

ORTIZ, M., SARABIA, L., SÁNCHEZ, M. & GIMENEZ, D. 2009. Identification and quantification of ciprofloxacin in urine through excitation-emission fluorescence and three-way PARAFAC calibration. *Analytica Chimica Acta,* 642**,** 193-205.

POGGIE, R. A., MISHRA, A. K. & DAVIDSON, J. A. 1994. Three body abrasive wear behaviour of orthopaedic implant bearing surfaces from titanium debris. *Journal of Materials Science: Materials in Medicine,* 5**,** 387-392.

POUDEL. 2013. *Frictional force* [Online]. Science HQ. Ed. Rod Pierce. Available: http://www.sciencehq.com/physics/frictional-force.html [Accessed 1 Oct 2013].

RABINOWICZ, E. 1965. *Friction and wear of materials*, Wiley New York.

RABINOWICZ, E. & MUTIS, A. 1965. Effect of abrasive particle size on wear. *Wear,* 8**,** 381-390.

ROUX, W., DU PREEZ, R. & STANDER, N. 1999. Design optimisation of a semi-solid tyre using response surface approximations. *Engineering Computations,* 16**,** 165-184.

ROYLANCE, B. 2003. Machine failure and its avoidance—what is tribology's contribution to effective maintenance of critical machinery? *Proceedings of the Institution of Mechanical Engineers, Part J: Journal of Engineering Tribology,* 217**,** 349-364.

RUAN, J.-A. & BHUSHAN, B. 1994. Atomic-scale friction measurements using friction force microscopy. I: General principles and new measurement techniques. *Journal of Tribology,* 116**,** 378-388.

SALIH, N., SALIMON, J., YOUSIF, E. & ABDULLAH, B. M. 2013. Biolubricant basestocks from chemically modified plant oils: ricinoleic acid based-tetraesters. *Chemistry Central Journal,* 7**,** 128.

SAW, S. K., SARKHEL, G. & CHOUDHURY, A. 2012. Preparation and characterization of chemically modified Jute–Coir hybrid fiber reinforced epoxy novolac composites. *Journal of Applied Polymer Science,* 125**,** 3038-3049.

SHAUGHNESSY, E. J., KATZ, I. M. & SCHAFFER, J. P. 2005. *Introduction to fluid mechanics*, Oxford University Press, USA.

SIMO, J. & LAURSEN, T. 1992. An augmented Lagrangian treatment of contact problems involving friction. *Computers & Structures,* 42**,** 97-116.

SıNMAZÇELIK, T. & TAŞKıRAN, İ. 2007. Erosive wear behaviour of polyphenylenesulphide (PPS) composites. *Materials & design,* 28**,** 2471-2477.

STACHOWIAK, G. & BATCHELOR, A. W. 2011. *Engineering tribology*, Butterworth-Heinemann.

WATTS, D. G. 1995. Understanding canonical analysis. *Journal of Quality Technology,* 27**,** 40-44.

WU, C. J. & HAMADA, M. 2000. Experiments: Planning. *Analysis, and Parameter Design Optimization. Wiley*.

ZHOU, X., SUN, Y. & WANG, W. 2009. Influences of carbon fabric/epoxy composites fabrication process on its friction and wear properties. *Journal of Materials Processing Technology,* 209**,** 4553-4557.

# University of southern Queensland

## Faculty of engineering and serving

**For**: Chris Snook

**Topic:** Respond surface Methodology (RMS)

**Supervisor**: Belal Yousif

**Enrolment**: ENG 4111 – s1

ENG 4112 - s2

**Project aim:** this project aim to develop empirical equation to simulate the wear and frictional properties of polymer.

**Programme:**

1. Search and learn about the background and applications of the respond surface methodology (RSM) and how to apply it on the experimental data.

2. Analyse the experimental data using the (RSM) to develop a relationship (equation) between the response and the independent variables.

3. The outcome of the work will contribute to the knowledge of tribology since; there is lack of work in the respond surface methodology area.

4. The outcome of the work will be published in an international journal related to the area of study.

5. Developing an empirical equation will assist to reduce the experimental time, so from this work a new empirical equation will be developed which going to be as a base for the researchers.

**As time permits:**

6. The derived empirical equation will be tested in the lab to physically check its accuracy.